

# Constraints on Yukawa gravity parameters from observations of bright stars

P. Jovanović,<sup>a,1</sup> V. Borka Jovanović,<sup>b</sup> D. Borka<sup>b</sup> and A. F. Zakharov<sup>c</sup>

<sup>a</sup>Astronomical Observatory, Volgina 7, P.O. Box 74, 11060 Belgrade, Serbia

<sup>b</sup>Department of Theoretical Physics and Condensed Matter Physics (020), Vinča Institute of Nuclear Sciences - National Institute of the Republic of Serbia, University of Belgrade, P.O. Box 522, 11001 Belgrade, Serbia

<sup>c</sup>Bogoliubov Laboratory for Theoretical Physics, JINR, 141980 Dubna, Russia

E-mail: [pjovanovic@aob.rs](mailto:pjovanovic@aob.rs), [vborka@vinca.rs](mailto:vborka@vinca.rs), [dusborka@vinca.rs](mailto:dusborka@vinca.rs),  
[alex.fed.zakharov@gmail.com](mailto:alex.fed.zakharov@gmail.com)

**Abstract.** In this paper we investigate a Yukawa gravity modification of the Newtonian gravitational potential in a weak field approximation. For that purpose we derived the corresponding equations of motion and used them to perform two-body simulations of the stellar orbits. In 2020 the GRAVITY Collaboration detected the orbital precession of the S2 star around the supermassive black hole (SMBH) at the Galactic Center (GC) and showed that it is close to the general relativity (GR) prediction. Using this observational fact, we evaluated parameters of the Yukawa gravity (the range of Yukawa interaction  $\Lambda$  and universal constant  $\delta$ ) with the Schwarzschild precession of the S-stars assuming that the observed values as indicated by the GRAVITY Collaboration will have a small deviation from GR prediction [1]. GR provides the most natural way to fit observational data for S-star orbits, however, their precessions can be fitted by Yukawa gravity. Our main goal was to study the possible influence of the strength of Yukawa interaction, i.e. the universal constant  $\delta$ , on the precessions of S-star orbits. We analyze S-star orbits assuming different strength of Yukawa interaction  $\delta$  and find that this parameter has strong influence on range of Yukawa interaction  $\Lambda$ . For that purpose we use parameterized post-Newtonian (PPN) equations of motion in order to calculate the simulated orbits of S-stars in GR and Yukawa gravity. Using MCMC simulations we obtain the best-fit values and uncertainties of Yukawa gravity parameters for S-stars. Also, we introduce a new criterion which can be used for classification of gravitational systems in this type of gravity, according to their scales. We demonstrated that performed analysis of the observed S-stars orbits around the GC in the frame of the Yukawa gravity represent a tool for constraining the Yukawa gravity parameters and probing the predictions of gravity theories.

---

<sup>1</sup>Corresponding author.

---

## Contents

<b>1</b>	<b>Introduction</b>	<b>1</b>
<b>2</b>	<b>Yukawa-like nonlinear correction to the gravitational potential</b>	<b>5</b>
<b>3</b>	<b>Analysis of the stellar orbits around Sgr A* in Yukawa gravity</b>	<b>6</b>
<b>4</b>	<b>Results and discussion</b>	<b>8</b>
4.1	Constrains on Yukawa gravity parameters from the stellar orbits around GC	8
4.2	Constrains on Yukawa gravity parameters from Markov chain Monte Carlo simulations	12
<b>5</b>	<b>Conclusions</b>	<b>17</b>

---

## 1 Introduction

General Relativity (GR) was introduced by A. Einstein in 1915 and consequent observations and experiments showed that GR is the best gravity model [2–4], since GR successfully passed all considered tests.

The Galactic Center (radio source Sgr A\*) is the closest galactic center. Astronomers believe that supermassive black hole (SMBH) is located at the Galactic Center (GC) as it was suggested in [5–7] however, many alternative models have been proposed for GC, including for instance a dense cluster of stars [8], fermion ball [9], boson stars [10–12], neutrino balls [13, 14] and others [15–18]. Recently, it was proposed to substitute the SMBH at GC by dark matter concentration with a dense core and diluted halo [20] and it was claimed that such an approach provides a better fit in comparison of the conventional approach where a SMBH is the key component [21]. However, a consequent analysis of the RAR-model (Ruffini, Arguelles, Rueda) showed that since in spite of the fact that trajectories of bright stars inside a ball with a constant density are elliptical their properties are different from observational ones [22, 23] and therefore, to fit trajectories of bright stars almost all dark matter mass has to be in a ball with a radius which is smaller than pericenters of these stars [24]. Therefore, many alternatives for SMBH were significantly constrained by consequent observations and SMBH is the most reliable and natural model for GC. The nearest SMBH is located in the center of our Galaxy; therefore, this object is very attractive for observations, and astronomers observe it in various spectral ranges, including gamma-ray, X-ray, infrared, optical and radio ranges.

About 50 years ago Bardeen [25] presented a picture of a dark region (a shadow) for a thought observation which corresponds to a bright screen located behind a Kerr black hole and a distant observer is located in the equatorial plane. Later, Chandrasekhar [26] reproduced a similar picture in his book. However, neither Bardeen nor Chandrasekhar did not consider shadow as a possible test of GR since a) shadow sizes are extremely small to be detected for known black holes and b) there are no bright screens precisely behind black hole in astronomy. In addition we would like to note that perhaps Bardeen and Chandrasekhar did not suggest to use the apparent shape of a black hole as GR test, because the dark region (shadow) is too small to be detectable for all known estimates of black hole masses and distances toward them. In papers [27, 28] the authors showed results of simulations of shadow formation for

the GC in the framework of a numerical model, where the authors took into account electron scattering for a radiation in mm and cm bands. The authors concluded that it is possible to observe a dark region (shadow) around the black hole in mm band, while it is not possible to see a shadow in cm band due to electron scattering. It was expected to create a global network acting in 1.3 mm wavelength, therefore the best angular resolution of this interferometer is around  $25 \mu\text{as}$  (similar to the current resolution of Event Horizon Telescope (EHT) network, while the shadow diameter was estimated as small as  $30 \mu\text{as}$  assuming that the black hole mass is  $2.6 \times 10^6 M_\odot$  as it was evaluated in [29, 30], therefore, expectations for shadow observations with these facilities were not very optimistic, however, now we know that the black hole mass is more than  $4 \times 10^6 M_\odot$  and EHT Collaboration reconstructed the shadow at Sgr A\* in 2022. Therefore, a problem of shadow reconstruction using EHT Collaboration observations is very hard but slightly simpler than it was expected in 2000.

At the beginning of this century, astrophysical problems were discussed for the Radioastron space telescope under construction; it was supposed to conduct simultaneous observations with ground based telescopes. The angular resolution of such an Earth–space interferometer could be of the order of 7 angular microseconds at the shortest wavelength of 1.3 cm. The mass of the black hole in the GC is about  $4 \times 10^6 M_\odot$ , and the distance to it is of the order of 8 kpc; thereby, the angular size of the Schwarzschild radius is  $10 \mu\text{as}$ , which turns out to be comparable with the angular resolution of the interferometer. It would seem that we could discuss manifestations of the general theory of relativity that could be detected. Assuming that the photons are only curved by the gravitational field of the black hole, but do not scatter near its vicinity, the size and shape of the shadow (that is, the dark area for the distant observer) was described in [31, 32]. This means that for the observer standing in the equatorial plane, the value of  $\theta$  is the same (it does not depend on the spin value), and the shadow is deformed in the direction parallel to the equatorial plane; the deformation depends on spin. Thus, the size of the shadow for the black hole in the GC is about  $50 \mu\text{as}$  and, in principle, the structures with such a size could be observed with the Radioastron. However, scientists subsequently understood that, apparently, the image shape is smeared due to the scattering of photons on electrons for the centimeter range, and in order to detect the shadow, it is necessary to switch to the millimeter and submillimeter wavelength ranges, i.e., to the wavelengths that are planned to be used in the designed Millimetron space interferometer, as noted in [31, 32]. An international global network of telescopes, including the millimeter wavelength range or the so-called the Event Horizon Telescope, operating as a giant interferometer the size of the Earth, observes the distribution of bright spots in the vicinity of the GC and determines the parameters of the black hole in the GC, and constrains alternative theories of gravity using this distribution. In April 2019, this team of scientists reported the first image of a supermassive black hole in the center of the M87 galaxy, which is located at a distance of about 17 Mpc from the Earth and the mass of the black hole in its center is (in April 2017, observations were made at a wavelength of 1.3 mm). The shadow size for this black hole is about  $42 \mu\text{as}$  [33], that is, the black hole in the center of the M87 galaxy is much more massive and it is located much farther than the GC, but their shadows are similar in size (this situation is somewhat similar that the angular sizes of the Sun and Moon visible from the Earth are very close in size) since it was shown recently by the EHT collaboration the shadow diameter for Sgr A\* is  $52 \mu\text{as}$  [34].

As it was noted earlier to evaluate the parameters of the gravitational potential in the GC, photons may be used as test particles (in this case, the size and shape of the shadow in the vicinity of the GC are analyzed). Also, the bright stars that move in the vicinity of the

black hole are used as test particles. Despite the fact that GR predictions are confirmed by the results of many observations and experiments (in particular, for the gravitational field in the vicinity of a black hole in the GC in 2018, the GRAVITY collaboration confirmed GR predictions about the gravitational redshift of the spectrum of star S2 near the pericenter passage on May 18, 2018 and these conclusions are in good agreement with the observations presented by the Keck team [1, 35–37]). Below we will use observations of bright star trajectories to constrain gravitational potential at Sgr A\*.

As the carrier of the gravitational interaction, graviton is considered to be spin-2 (tensor) boson, electrically uncharged, as well as massless since, according to GR, it travels along null geodesics at the speed of light  $c$  (like photon). However, according to some alternative theories, gravity is propagated by a massive field, i.e. by a graviton with some small, nonzero mass  $m_g$ . For detailed reviews on massive gravity including theories without ghosts see [38–40] and references therein (earlier, a presence of Boulware – Deser [41] ghosts was considered as a significant pathology of massive gravity theories). Ever since they were first introduced by Fierz and Pauli in 1939 [42], such so called theories of massive gravity have gained a significant attention due to their ability to provide a possible explanation for the accelerated expansion of the Universe without dark energy (DE) hypothesis, and due to important predictions that the velocity of gravitational waves (gravitons) should depend on their frequency, as well as that the effective gravitational potential should include a nonlinear (exponential) correction of Yukawa form, depending on the Compton wavelength of graviton:  $\lambda_g = h/(m_g c)$ . Namely, if gravitation is propagated by a massive field, then the effective Newtonian potential has a Yukawa form:  $\propto r^{-1} \exp(-r/\lambda_g)$ , and the massive graviton then propagates at an energy  $E$  (or frequency  $f$ ) dependent speed:  $v_g^2/c^2 = 1 - m_g^2 c^4/E^2 = 1 - h^2 c^2/(\lambda_g^2 E^2) = 1 - c^2/(f \lambda_g)^2$  [43, 44]. The above modified dispersion relation is obtained from the modified special relativistic relation between energy  $E$  and momentum  $p$  of graviton:  $E^2 = p^2 c^2 + m_g^2 c^4$ , and by taking that its velocity  $v_g$  satisfies:  $v_g^2/c^2 \equiv c^2 p^2/E^2$ . Moreover, one can obtain the observational constraints on the  $v_g/c$  ratio from the time difference  $\Delta t \equiv \Delta t_a - (1+z)\Delta t_e$  between a gravitational wave and an electromagnetic wave from the same event, where  $\Delta t_a$  and  $\Delta t_e$  are the differences in arrival time and emission time, respectively, of these two signals, and  $z$  is the redshift of the source [43]. The fractional speed difference can be then obtained using the following expression:  $1 - \frac{v_g}{c} = 5 \times 10^{-17} \left( \frac{200 \text{ Mpc}}{D} \right) \left( \frac{\Delta t}{1 \text{ s}} \right)$ , where  $D$  is distance of the source [43, 44].

Below we present a short overview of observational tests of massive gravity theories, and their applications for obtaining the constraints on Compton wavelength and mass of graviton, as well as on speed of gravity (for more detailed review see e.g. [39]).

Yukawa-like potential of the form  $U(r) = \frac{G_\infty M}{r} \left( 1 + \alpha e^{-r/r_0} \right)$  was studied in [45], where  $\alpha$  is the strength of Yukawa interaction,  $r_0$  is a characteristic length scale, while the gravitational constant measured locally ( $G_0$ ) and at infinity ( $G_\infty$ ) are related by:  $G_0 = G_\infty (1 + \alpha)$ . It was found that, if the length scale  $r_0$  corresponds to graviton mass  $m_0$  as  $r_0 = \frac{h}{m_0 c}$ , then the flat rotation curves of spiral galaxies could be accounted for  $\alpha \sim -1$  and without introducing dark matter (DM) hypothesis [45]. The negative sign of the strength of Yukawa interaction  $\alpha$  indicated an additional repulsive (anti-gravity) force which could mimic the effects of dark energy on the large scales. Thus, it was demonstrated that this type of correction on gravitational potential could be used to account for both DM at galactic and DE at cosmological scales, which is one of the main reasons while Yukawa gravity has recently

attracted the significant attention.

Different experimental tests and constraints on the range and strength of additional Yukawa gravitational interaction between masses  $m_1$  and  $m_2$  in the form  $V(r) = -G_N \frac{m_1 m_2}{r} (1 + \alpha e^{-r/\lambda})$  were reviewed in [46]. These constraints covered a wide range of length scales, including short-range laboratory experiments with torsion balance, lunar laser ranging (LLR) and Solar System tests, and were summarized in Figs. 9 and 10 of [46]. In the case of LLR and Solar System, the following constraints on the range of Yukawa interaction  $\Lambda$  were obtained, respectively:  $\lambda \gg 4 \times 10^8$  m and  $\lambda \gg 1.5 \times 10^{11}$  m.

LIGO Scientific and Virgo Collaborations used the following Yukawa type correction to the gravitational potential with characteristic length scale  $\lambda_g$ :  $\varphi(r) = \frac{GM}{r} (1 - e^{-r/\lambda_g})$  in order to discuss and compare the so-called static and dynamical bounds on graviton mass [47]. In the first publication on the discovery of gravitational waves and binary black holes the authors found a graviton mass constraint from a dispersion relation therefore, a massive gravity theory was considered as feasible alternative for GR. The static bounds, such as those from the Solar System observations, do not probe the propagation of gravitational interaction, in contrast to dynamical bounds which are obtained by studying the very massive, compact objects such as binary pulsars and supermassive Kerr black holes. Fig. 8 of [48] shows a comparison of cumulative posterior probability distribution and exclusion regions for the graviton Compton wavelength, obtained from the first gravitational wave signal GW150914 with exclusion regions obtained from the binary pulsar J0737-3039 and the Solar System observations. The resulting dynamical bound of  $\lambda_g > 10^{13}$  km at 90% confidence, which corresponds to a graviton mass  $m_g \leq 1.2 \times 10^{-22}$  eV, obtained from GW150914, was approximately for a factor of three better than the existing Solar-System static bounds [48] (after data analysis of the third working run LIGO–Virgo–KAGRA consortium improved previous estimates as  $m_g \leq 1.27 \times 10^{-23}$  eV [49]). This LIGO–Virgo bound on graviton mass is currently considered as the most robust, although some other techniques could in principle provide more stringent constraints. For example, expected detection limit for a future pulsar timing array (PTA) with 300 pulsars, observed for 10 years is  $m_g = 5 \times 10^{-23}$  eV [50] (however, here we should emphasize that we compare the found graviton mass bounds from gravitational wave observations and constraints which will be expected to find from future pulsar timing observations), while the current studies of weak lensing, which are model-dependent and very sensitive to the uncertainties on the amount and spatial distribution of DM in the Universe, provide the limit of  $\lambda_g > 6.82$  Mpc which corresponds to  $m_g < 6 \times 10^{-30}$  eV [51].

However, further progress in tightening the bound on  $\lambda_g$  (and thus on the graviton mass) was recently achieved using Solar system data on the perihelion advance of planets from Mercury to Saturn, obtained by high-precision radar tracking of planets and spacecrafts, as well as using improved ephemeris computer codes [52]. Assuming the Newtonian gravitational potential given by the Yukawa form  $(Gm/r)e^{-r/\lambda_g}$ , the following approximate expression (up to leading order in  $a/\lambda_g$  ratio) for the perihelion advance per orbit was obtained:  $\Delta\varpi \approx \pi \left(\frac{a}{\lambda_g}\right)^2 (1 - e^2)^{-1/2}$ , where  $\varpi$  is the longitude of perihelion,  $a$  is the orbital semimajor axis and  $e$  is the orbital eccentricity [52]. The resulting lower bound on  $\lambda_g$  was between 1.2 and  $2.2 \times 10^{14}$  km (see Table 1 in [52]), surpassing the first LIGO/Virgo graviton bounds by an order of magnitude.

Recently, there has been also an attempt to constrain the speed of gravity from the ob-

served time difference between gravitational wave event GW170817, observed by the Advanced LIGO and Virgo detectors, and  $\gamma$ -ray burst GRB170817A, observed independently by  $\gamma$ -ray detectors onboard the Fermi and the International Gamma-Ray Astrophysics Laboratory (INTEGRAL) space observatories [53]. These two GW and  $\gamma$ -ray signals were emitted from a binary neutron star merger in the nearby galaxy NGC 4993, located at redshift  $z \approx 0.01$ , which corresponds to the luminosity distance of  $D = 26$  Mpc. Optical and IR telescopes (Swope, DLT40, MASTER, DECam, VISTA et al.) played a crucial role for the localization of the event and a power of multi-messenger astronomy was remarkably demonstrated [54]. The observed time difference between GRB 170817A and GW170817 was  $1.74 \pm 0.05$  s, while their emitted time difference was unknown [53]. Therefore, the upper and lower bounds on speed of gravity were estimated assuming that the peak of the gravitational wave signal and the first  $\gamma$ -photons were emitted simultaneously (i.e. by attributing the entire observed lag to the faster gravitational wave signal), and that  $\gamma$ -ray signal was emitted 10 s after the gravitational wave signal, respectively. This resulted with the following constraint on the fractional speed difference:  $-3 \times 10^{-15} \leq \frac{v_g}{c} - 1 \leq +7 \times 10^{-16}$  [53].

This research is continuation of our previous investigations in this field [55–63], in which we constrained the parameters of Yukawa gravity using the observed stellar orbits around the central SMBH of the Milky Way [64–71], as well as developed a novel and independent method for obtaining the graviton mass bounds from these observations which are, since 2019, accepted by the Particle Data Group (PDG) and included in their "Gauge and Higgs Boson Particle Listings" [72]. In addition, here we will extend our study on the possible influence of the strength of Yukawa interaction, described by the parameter  $\delta$  in the gravitational potential, on the obtained bounds on graviton mass. This paper is organized as follows: in §2 we present the procedure for obtaining the gravitational potential with a Yukawa-like correction in the Newtonian limit of any analytic  $f(R)$  gravity model, in §3 we describe some basic properties of S-stars and their observed orbits around the SMBH at GC, as well as our method for obtaining the Compton wavelength and graviton mass from analysis of the observed stellar orbits in Yukawa gravity, in §4 we discuss the main results of our study, especially regarding the strength of Yukawa interaction  $\delta$ , and finally in §5 we point out of our most important conclusions.

## 2 Yukawa-like nonlinear correction to the gravitational potential

Yukawa-like potentials are characterized by presence of decreasing exponential terms and that's why deviate from the standard Newtonian gravitational potential [45, 73–77].

The Yukawa term is analysed in case of short and long ranges. The Yukawa term for the short ranges is analysed in [46] and references therein, and for the longer ranges the parameters of Yukawa gravity potential are given for clusters of galaxies [78, 79], for rotation curves of spiral galaxies [75] and for the binary pulsars [80, 81]. Also, other studies of long-range Yukawa term investigations can be found in [74, 82–87].

The action of Yukawa-like nonlinear correction to the gravitational potential in the Newtonian limit can be given in the form [56]:

$$\mathcal{S} = \int d^4x \sqrt{-g} [f(R) + \mathcal{X} \mathcal{L}_m], \quad \mathcal{X} = \frac{16\pi G}{c^4}, \quad (2.1)$$

where  $f$  is a generic function of Ricci scalar curvature  $R$  and  $\mathcal{X}$  is the coupling constant.



The resulting 4<sup>th</sup>-order field equations are following:

$$f'(R)R_{\mu\nu} - \frac{1}{2}f(R)g_{\mu\nu} - f'(R)_{;\mu\nu} + g_{\mu\nu}\square f'(R) = \frac{\mathcal{X}}{2}T_{\mu\nu}. \quad (2.2)$$

Trace of these equations is given by:

$$3\square f'(R) + f'(R)R - 2f(R) = \frac{\mathcal{X}}{2}T. \quad (2.3)$$

Expansion of analytic Taylor expandable  $f(R)$  functions with respect to the value  $R = 0$  (i.e. around the Minkowskian background) has the following form:

$$f(R) = \sum_{n=0}^{\infty} \frac{f^{(n)}(0)}{n!} R^n = f_0 + f_1 R + \frac{f_2}{2} R^2 + \dots \quad (2.4)$$

By adopting the spherical symmetry, the metric can be recast as follows [88]:

$$ds^2 = \left[1 + \frac{2\Phi(r)}{c^2}\right] c^2 dt^2 - \left[1 - \frac{2\Psi(r)}{c^2}\right] dr^2 - r^2 d\Omega^2, \quad (2.5)$$

where  $\Phi(r)$  and  $\Psi(r)$  are two potentials given by [56, 88]:

$$\Phi(r) = -\frac{GM}{(1+\delta)r} \left(1 + \delta e^{-\frac{r}{\Lambda}}\right), \quad (2.6)$$

$$\Psi(r) = \frac{GM}{(1+\delta)r} \left[\left(1 + \frac{r}{\Lambda}\right) \delta e^{-\frac{r}{\Lambda}} - 1\right]. \quad (2.7)$$

The parameter  $\Lambda$  is the range of interaction ( $\Lambda^2 = -f_1/f_2$ ) and depends on the typical scale of a gravitational system. The second parameter  $\delta$  is the strength of interaction ( $\delta = f_1 - 1$ ).

In our previous investigations we constrained different Extended Gravity theories using astronomical data for different astrophysical systems: the S2 star orbit [55, 57, 58, 62, 89–93], fundamental plane of elliptical galaxies [94–96] and baryonic Tully-Fischer relation of spiral galaxies [97]. Here, we analyse stellar orbits (so called S-stars) around the central SMBH of the Milky Way in the frame of Yukawa gravity in order to constrain gravity parameters [55–63].

### 3 Analysis of the stellar orbits around Sgr A\* in Yukawa gravity

S-stars are the bright stars which move around the GC [1, 64–71, 98–101] where a compact bright radio source Sgr A\* is located. The GC consists of the SMBH with mass around  $4.3 \times 10^6 M_\odot$  and an extended mass distribution formed with stellar cluster, interstellar and probably dark matter. We assume that total mass of bulk distribution inside a spherical shell where trajectories of bright stars are located is much smaller than the BH mass and recent estimates done by the GRAVITY collaboration support these assumptions since for feasible density profiles the total extended mass inside a ball with the S2 apocenter radius must be less than  $3000 M_\odot$  at  $1 \sigma$  confidence level [102]. Also, using observations in May 2018, GRAVITY Collaboration [35, 36] and the Keck group [37] evaluated relativistic redshifts of spectral lines for the S2 star near its periapsis passage. The obtained results showed that the redshifts were

consistent with theoretical estimates done in the first post-Newtonian correction of GR. The orbits of S-stars around Sgr A\* are monitored for about 30 years by the following telescopes: New Technology Telescope and Very Large Telescope (NTT/VLT) in Chile [65, 66] (recently VLT units started to act as the GRAVITY interferometer) and by Keck telescopes in Hawaii [64]. These two groups performed the precise astrometric observations of S2 star. Nowadays, there are more recent and precise observations not only of S2 star, but also of several other members of the S-star cluster, such as S38, S55 and S62 [35, 67, 103, 104] and thus it is possible to perform the orbital analysis of these stars (see e.g. [105–115]).

We assume that S-stars move around the central SMBH of our Galaxy at a sufficiently large distances where the space-time is practically flat, and we studied the PPN equations of motion in both Yukawa gravity and GR. Besides the well known first post-Newtonian correction of GR, PPN equations of motion in Yukawa gravity also include an additional exponential correction which arises because the  $f(R)$  theories of gravity with Yukawa-like potentials do not entirely fit into the standard PPN formalism and require its extension/modification (see e.g. [116, 117] and references therein). Therefore, in this modified PPN formalism the equations of motion in Yukawa gravity have the following form:

$$\vec{r}_Y = \vec{r}_N + \vec{r}_{cor,PPN} + \vec{r}_{cor,Y}, \quad (3.1)$$

where the  $\vec{r}_N$  is the Newtonian acceleration,  $\vec{r}_{cor,PPN}$  is its first post-Newtonian correction in the PPN formalism and  $\vec{r}_{cor,Y}$  is additional Yukawa correction. These three contributions are given by the following expressions (see Eq. (2.1) from Ref. [81]):

$$\begin{aligned} \vec{r}_N &= -GM \frac{\vec{r}}{r^3} \\ \vec{r}_{cor,PPN} &= \frac{GM}{c^2 r^3} \left\{ \left[ 2(\beta + \gamma) \frac{GM}{r} - \gamma (\vec{r} \cdot \vec{r}) \right] \vec{r} + 2(1 + \gamma) (\vec{r} \cdot \vec{r}) \vec{r} \right\} \\ \vec{r}_{cor,Y} &= \frac{\delta \cdot GM}{1 + \delta} \left[ 1 - \left( 1 - \frac{r}{\Lambda} \right) e^{-\frac{r}{\Lambda}} \right] \frac{\vec{r}}{r^3}. \end{aligned} \quad (3.2)$$

The standard PPN equations of motion in the GR case are given by:

$$\vec{r}_{GR} = \vec{r}_N + \vec{r}_{cor,PPN}. \quad (3.3)$$

Simulated orbits of S-stars in Yukawa gravity and GR were then obtained by numerical integration of the expressions (3.1) and (3.3), respectively. Both  $\beta$  and  $\gamma$  PPN parameters in  $\vec{r}_{cor,PPN}$  are taken to be equal to 1, since Yukawa gravity is indistinguishable from GR up to the first post-Newtonian correction [116]. The obtained results are used for studying the orbital precession caused by Yukawa type correction in the gravitational potential and mutual comparisons between the orbits simulated in Yukawa gravity and in GR.

In this paper we also assumed that the orbital precession of the S-stars is close to the corresponding GR prediction and only slightly deviates from it. This assumption was based on the fact that the GRAVITY Collaboration detected the orbital precession of the S2 star around the SMBH and showed that it was close to the corresponding prediction of GR [1]. Taking this into account, we derived expression for parameter  $\Lambda$  under an assumption that the orbital precession of S-stars in Yukawa gravity deviates from the Schwarzschild precession in GR by a specific factor  $f_{SP} = 1.10$ , as indicated in [1].



The approximate formula for the additional contribution of Yukawa gravity to the Schwarzschild precession for  $a \ll \Lambda$  is [58]:

$$\Delta\varphi_Y^{rad} \approx \frac{\pi\delta\sqrt{1-e^2}}{1+\delta} \frac{a^2}{\Lambda^2}, \quad (3.4)$$

where  $e$  is orbital eccentricity and  $a$  is the semi-major axis of the orbital ellipse. The total orbital precession can be obtained by adding the above expression to the formula for Schwarzschild precession [44]:

$$\Delta\varphi_{GR}^{rad} \approx \frac{6\pi GM}{c^2 a(1-e^2)}, \quad (3.5)$$

and it is expected to be close to the observed precession:

$$\Delta\varphi_Y + \Delta\varphi_{GR} \approx \Delta\varphi_{obs}, \quad (3.6)$$

where  $\Delta\varphi_Y$ ,  $\Delta\varphi_{GR}$  and  $\Delta\varphi_{obs}$  are Yukawa contribution, GR contribution and observed precession [1], respectively. This can be recast as:

$$\frac{2\delta\sqrt{1-e^2}}{1+\delta} \frac{a^2}{\Lambda^2} + \frac{6\pi GM}{c^2 a(1-e^2)} \approx \frac{2\pi GM}{c^2 a(1-e^2)} (3f_{sp}), \quad (3.7)$$

where parameter  $f_{sp}$  is defined as:  $f_{sp} = \frac{2+2\gamma-\beta}{3}$ , and it characterizes how relativistic the model is. The value of  $f_{sp} = 1.10 \pm 0.19$  was measured by GRAVITY Collaboration [1]. Using the third Kepler law (since the orbits are very close to Newtonian ones):

$$\frac{P^2}{a^3} \approx \frac{4\pi^2}{GM}, \quad (3.8)$$

it was found that, according to the expression (3.7),  $\Lambda$  has to satisfy the following condition:

$$\Lambda(P, e; \delta) \approx \frac{cP}{2\pi} \sqrt{\frac{\delta(\sqrt{1-e^2})^3}{2(3f_{sp}-3)(1+\delta)}}. \quad (3.9)$$

We can see that for the given values of universal constant  $\delta$  and parameter  $f_{sp}$ , the following condition holds:  $\Lambda \propto cP^*$ , where  $P^* = P(1-e^2)^{3/4}$ . Thus,  $P^*$  can be used as a criterion for classification of the gravitational systems according to their scales, as well as to find the systems which could be described by similar values of the range of Yukawa interaction  $\Lambda$ .

## 4 Results and discussion

### 4.1 Constrains on Yukawa gravity parameters from the stellar orbits around GC

In order to study the influence of strength of Yukawa interaction  $\delta$  on its range  $\Lambda$  in the case of different S-stars, we estimated the values of  $\Lambda$  and its absolute errors for the following three values of  $\delta$ :  $\delta = 0.1, \delta = 10$  and  $\delta = 100$ . The obtained estimates are given in Tables 1 and 2 in which the following values are given for each S-star: orbital precession ( $\Delta\varphi$ ), scale criterion  $P^* = P(1-e^2)^{3/4}$ , range of Yukawa interaction ( $\Lambda$ ) and its absolute error ( $\Delta\Lambda$ ). The observed orbital elements and their uncertainties are taken from Table 3 of [67] for all given S-stars, except of S111. It can be seen from Tables 1 and 2 that universal constant  $\delta$

strongly affects the range of Yukawa interaction  $\Lambda$  and that they are correlated in the case of weaker Yukawa interaction (i.e. for smaller values of  $\delta$ , such as  $\delta = 0.1$ ).

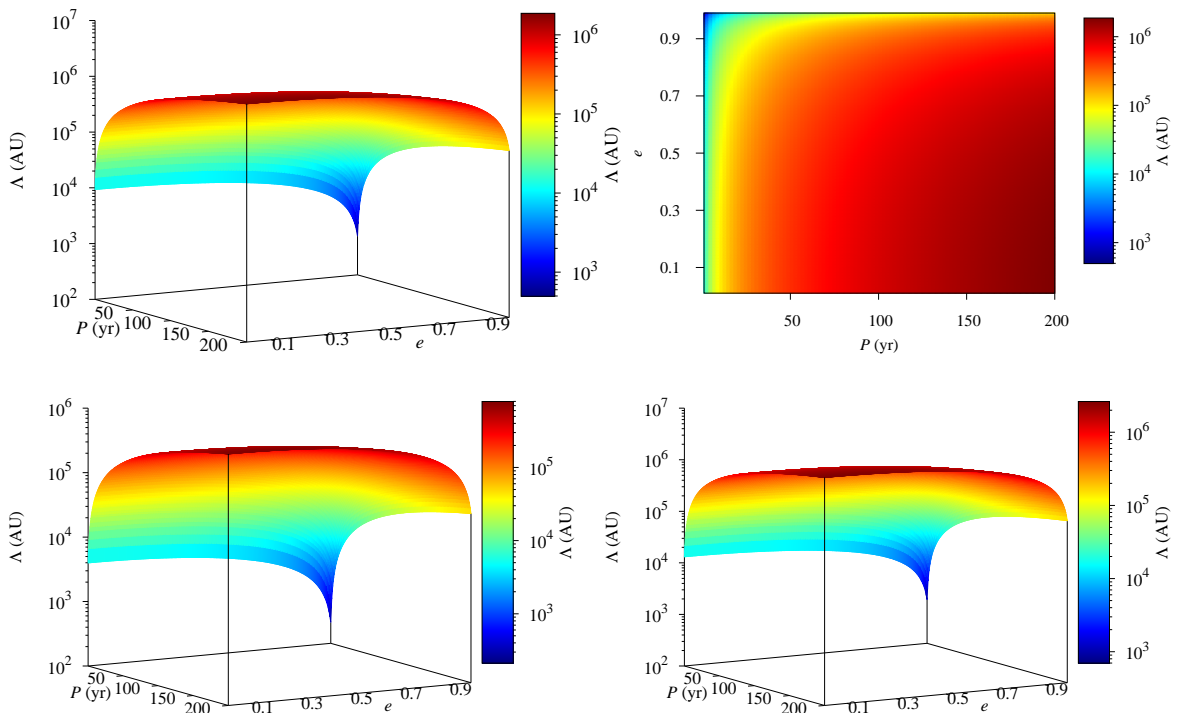


**Figure 1.** The 3D graphic (top left) of the function  $\Lambda(P, e)$  defined in (3.6) and representing the dependence of the range of Yukawa interaction  $\Lambda$  on the orbital period  $P$  (yr) and eccentricity  $e$  of S-stars for  $\delta = 1$ , as well as its projection to the  $P - e$  parameter space (top right). Bottom panels shows the same as in top left panel, but for  $\delta = 0.1$  (bottom left) and  $\delta = 100$  (bottom right).

Effects of 4 different values of parameter  $\delta$  (0.1, 1, 10 and 100) on estimates of parameter  $\Lambda$ , are presented in Figs. 1-2. Several 3D graphics of the function  $\Lambda(P, e)$ , representing  $\Lambda$  dependence on orbital period  $P$  (yr) and eccentricity  $e$  of S-stars, are shown in Fig. 1 (see also Tables 1 and 2 for some particular S-stars). Top panels of Fig. 1 show the case for  $\delta = 1$ , while the bottom panels present two cases:  $\delta = 0.1$  (bottom left) and  $\delta = 100$  (bottom right). From Fig. 1 it is evident that the larger values for the  $\Lambda$  are obtained for the S-stars with larger orbital periods  $P$  and lower eccentricities  $e$ . The shape of surface which represents the values of the  $\Lambda$  is similar for all studied values of  $\delta$ , but the values of  $\Lambda$  are different for different values of Yukawa strengths  $\delta$ . In the case of  $\delta = 1$ , the values for  $\Lambda$  are ranging from  $10^4$  to  $10^6$  AU (see Fig. 1). Especially, this difference is noticeable if one compares the case for  $\delta = 0.1$  with other studied cases.

The dependence of the gravity range parameter  $\Lambda$  on the observed orbital periods  $P$  and eccentricities  $e$  of a number of S-stars is shown in Fig. 2 for 4 different values of parameter  $\delta$ :  $\delta = 0.1, 1, 10$  and  $100$ , respectively (see also Table 1). Like in Fig. 1, it is evident that the larger values of  $\Lambda$  are obtained for S-stars with larger orbital periods  $P$  and lower eccentricities  $e$  as it follows from Eq. (3.9). We can see that the estimate of  $\Lambda$  is very sensitive to the value of Yukawa strength parameter  $\delta$ , and that the larger values of  $\Lambda$  are obtained for higher values of  $\delta$ . For  $\delta \gtrsim 10$ , there is very small influence on  $\Lambda$  compared to case  $\delta = 1$ . Also, we can conclude that the gravity parameters  $\delta$  and  $\Lambda$  are mutually dependent only for

**Table 1.** Orbital precession ( $\Delta\varphi$ ), scale criterion ( $P^*$ ) for S-stars, range of Yukawa interaction ( $\Lambda$ ) and its absolute errors ( $\Delta\Lambda$ ). The range of Yukawa interaction and its absolute errors are estimated for the following three values of  $\delta$ :  $\delta = 0.01, \delta = 0.1$  and  $\delta = 1$ . The observed orbital elements and their uncertainties are taken from Table 3 of [67] for all given S-stars, except of S111.

Star	$\Delta\varphi$ ( $''$ )	$P^*$ (yr)	$\Lambda \pm \Delta\Lambda$ (AU)		
			$\delta = 0.01$	$\delta = 0.1$	$\delta = 1$
S1	48.2	125.79	164626.9 $\pm$ 13537.8	498844.4 $\pm$ 41021.7	1169893.8 $\pm$ 96204.5
S2	722.1	5.12	6730.8 $\pm$ 149.9	20395.2 $\pm$ 454.3	47831.0 $\pm$ 1065.4
S4	65.5	68.01	89185.0 $\pm$ 1750.2	270244.0 $\pm$ 5303.3	633778.4 $\pm$ 12437.2
S6	102.4	76.74	100839.1 $\pm$ 267.5	305557.6 $\pm$ 810.6	716596.2 $\pm$ 1901.1
S8	138.0	42.73	56050.5 $\pm$ 1717.2	169841.6 $\pm$ 5203.5	398314.0 $\pm$ 12203.2
S9	124.3	34.33	45030.4 $\pm$ 2503.1	136448.8 $\pm$ 7584.9	320000.8 $\pm$ 17788.2
S12	314.6	18.33	24050.7 $\pm$ 475.7	72877.1 $\pm$ 1441.4	170912.0 $\pm$ 3380.4
S13	91.6	42.20	55328.1 $\pm$ 601.8	167652.4 $\pm$ 1823.5	393179.8 $\pm$ 4276.6
S14	1465.9	5.60	7346.3 $\pm$ 981.2	22260.4 $\pm$ 2973.2	52205.2 $\pm$ 6972.8
S17	66.1	67.35	88370.7 $\pm$ 4262.7	267776.5 $\pm$ 12916.7	627991.6 $\pm$ 30292.4
S18	107.1	34.71	45506.5 $\pm$ 926.2	137891.7 $\pm$ 2806.5	323384.7 $\pm$ 6581.8
S19	87.1	72.62	95481.5 $\pm$ 36447.7	289323.6 $\pm$ 110442.1	678523.9 $\pm$ 259009.7
S21	217.4	19.18	25142.3 $\pm$ 1261.7	76185.0 $\pm$ 3823.2	178669.6 $\pm$ 8966.2
S22	19.0	456.10	599449.8 $\pm$ 236689.3	1816423.7 $\pm$ 717204.5	4259891.2 $\pm$ 1681993.5
S23	114.1	34.54	45425.0 $\pm$ 11014.4	137644.5 $\pm$ 33375.3	322805.0 $\pm$ 78272.1
S24	107.5	97.28	127590.2 $\pm$ 14036.6	386617.6 $\pm$ 42533.2	906698.7 $\pm$ 99749.1
S29	98.5	57.33	75236.9 $\pm$ 14099.5	227979.3 $\pm$ 42723.7	534658.8 $\pm$ 100196.0
S31	63.3	82.46	108733.3 $\pm$ 3953.7	329478.4 $\pm$ 11980.3	772695.3 $\pm$ 28096.4
S33	47.9	135.83	178323.3 $\pm$ 27097.8	540346.5 $\pm$ 82110.5	1267224.9 $\pm$ 192566.2
S38	427.5	8.31	10917.4 $\pm$ 51.8	33081.5 $\pm$ 157.1	77582.9 $\pm$ 368.4
S39	364.5	19.25	25286.5 $\pm$ 2038.3	76622.1 $\pm$ 6176.3	179694.7 $\pm$ 14484.7
S42	30.8	250.45	327668.0 $\pm$ 127216.9	992883.5 $\pm$ 385486.4	2328518.3 $\pm$ 904045.8
S54	81.5	144.02	187868.3 $\pm$ 301214.1	569269.5 $\pm$ 912724.3	1335055.3 $\pm$ 2140528.3
S55	382.8	7.38	9666.0 $\pm$ 302.1	29289.4 $\pm$ 915.3	68689.7 $\pm$ 2146.6
S60	105.5	50.59	66370.5 $\pm$ 2549.6	201112.8 $\pm$ 7725.8	471651.3 $\pm$ 18118.6
S66	13.4	655.82	860607.2 $\pm$ 88872.3	2607770.2 $\pm$ 269296.7	6115763.2 $\pm$ 631556.7
S67	19.3	402.94	528751.9 $\pm$ 32803.8	1602198.3 $\pm$ 99400.4	3757488.1 $\pm$ 233114.5
S71	106.2	100.28	131669.4 $\pm$ 20154.0	398978.3 $\pm$ 61069.7	935687.0 $\pm$ 143221.2
S83	15.3	589.30	773374.9 $\pm$ 184565.2	2343443.1 $\pm$ 559260.5	5495861.3 $\pm$ 1311582.1
S85	11.0	1772.21	2311796.7 $\pm$ 3523752.4	7005094.4 $\pm$ 10677503.5	16428402.6 $\pm$ 25040965.4
S87	7.6	1577.89	2065566.0 $\pm$ 200654.2	6258978.1 $\pm$ 608012.7	14678604.7 $\pm$ 1425916.1
S89	31.0	273.90	358908.7 $\pm$ 49485.2	1087547.9 $\pm$ 149947.8	2550525.9 $\pm$ 351658.7
S91	11.4	891.25	1168818.2 $\pm$ 101284.2	3541696.1 $\pm$ 306906.4	8306013.7 $\pm$ 719759.3
S96	13.6	646.91	848925.2 $\pm$ 53447.7	2572372.1 $\pm$ 161954.7	6032747.3 $\pm$ 379817.5
S97	9.7	1151.43	1516520.2 $\pm$ 550839.2	4595286.1 $\pm$ 1669126.3	10776901.1 $\pm$ 3914448.1
S145	23.6	343.33	452172.2 $\pm$ 222048.9	1370150.3 $\pm$ 672841.7	3213287.3 $\pm$ 1577953.6
S175	1812.0	6.30	8263.6 $\pm$ 2000.9	25040.0 $\pm$ 6062.9	58723.9 $\pm$ 14218.7
R34	18.6	589.73	775088.0 $\pm$ 220322.6	2348634.1 $\pm$ 667611.0	5508035.2 $\pm$ 1565686.6
R44	5.5	2579.33	3444472.6 $\pm$ 2260986.2	10437273.8 $\pm$ 6851130.7	24477576.8 $\pm$ 16067325.7

**Table 2.** The same as Table 1, but for the following three values of  $\delta$ :  $\delta = 10$ ,  $\delta = 100$  and  $\delta = 1000$ .

Star	$\Delta\varphi$ ( $''$ )	$P^*$ (yr)	$\Lambda \pm \Delta\Lambda$ (AU)		
			$\delta = 10$	$\delta = 100$	$\delta = 1000$
S1	48.2	125.79	1577484.5 $\pm$ 129722.1	1646268.8 $\pm$ 135378.5	1653653.1 $\pm$ 135985.7
S2	722.1	5.12	64495.3 $\pm$ 1436.6	67307.6 $\pm$ 1499.2	67609.5 $\pm$ 1506.0
S4	65.5	68.01	854586.6 $\pm$ 16770.4	891849.8 $\pm$ 17501.6	895850.2 $\pm$ 17580.1
S6	102.4	76.74	966258.1 $\pm$ 2563.5	1008390.6 $\pm$ 2675.3	1012913.7 $\pm$ 2687.3
S8	138.0	42.73	537086.4 $\pm$ 16454.8	560505.5 $\pm$ 17172.3	563019.6 $\pm$ 17249.3
S9	124.3	34.33	431489.0 $\pm$ 23985.5	450303.6 $\pm$ 25031.4	452323.4 $\pm$ 25143.7
S12	314.6	18.33	230457.7 $\pm$ 4558.1	240506.5 $\pm$ 4756.8	241585.3 $\pm$ 4778.2
S13	91.6	42.20	530163.5 $\pm$ 5766.6	553280.7 $\pm$ 6018.0	555762.4 $\pm$ 6045.0
S14	1465.9	5.60	70393.5 $\pm$ 9402.2	73462.9 $\pm$ 9812.1	73792.4 $\pm$ 9856.1
S17	66.1	67.35	846783.7 $\pm$ 40846.2	883706.7 $\pm$ 42627.3	887670.5 $\pm$ 42818.5
S18	107.1	34.71	436051.9 $\pm$ 8874.8	455065.4 $\pm$ 9261.8	457106.6 $\pm$ 9303.4
S19	87.1	72.62	914921.4 $\pm$ 349248.6	954815.5 $\pm$ 364477.2	959098.2 $\pm$ 366112.0
S21	217.4	19.18	240918.1 $\pm$ 12090.0	251423.0 $\pm$ 12617.2	252550.7 $\pm$ 12673.7
S22	19.0	456.10	5744036.1 $\pm$ 2267999.6	5994498.0 $\pm$ 2366893.0	6021386.0 $\pm$ 2377509.6
S23	114.1	34.54	435270.2 $\pm$ 105542.1	454249.7 $\pm$ 110144.2	456287.2 $\pm$ 110638.2
S24	107.5	97.28	1222592.3 $\pm$ 134501.7	1275901.9 $\pm$ 140366.5	1281624.9 $\pm$ 140996.1
S29	98.5	57.33	720933.8 $\pm$ 135104.2	752369.2 $\pm$ 140995.3	755743.9 $\pm$ 141627.7
S31	63.3	82.46	1041902.1 $\pm$ 37885.2	1087333.0 $\pm$ 39537.1	1092210.2 $\pm$ 39714.5
S33	47.9	135.83	1708725.8 $\pm$ 259656.2	1783232.7 $\pm$ 270978.2	1791231.3 $\pm$ 272193.7
S38	427.5	8.31	104612.8 $\pm$ 496.8	109174.3 $\pm$ 518.4	109664.0 $\pm$ 520.7
S39	364.5	19.25	242300.3 $\pm$ 19531.2	252865.5 $\pm$ 20382.8	253999.7 $\pm$ 20474.2
S42	30.8	250.45	3139773.4 $\pm$ 1219015.1	3276679.5 $\pm$ 1272168.8	3291376.9 $\pm$ 1277875.0
S54	81.5	144.02	1800188.1 $\pm$ 2886287.8	1878683.2 $\pm$ 3012140.9	1887109.9 $\pm$ 3025651.7
S55	382.8	7.38	92621.1 $\pm$ 2894.4	96659.7 $\pm$ 3020.7	97093.3 $\pm$ 3034.2
S60	105.5	50.59	635974.4 $\pm$ 24431.1	663705.3 $\pm$ 25496.4	666682.4 $\pm$ 25610.8
S66	13.4	655.82	8246493.5 $\pm$ 851590.8	8606072.0 $\pm$ 888723.4	8644674.1 $\pm$ 892709.7
S67	19.3	402.94	5066595.9 $\pm$ 314331.6	5287518.8 $\pm$ 328037.6	5311235.7 $\pm$ 329509.0
S71	106.2	100.28	1261680.1 $\pm$ 193119.5	1316694.1 $\pm$ 201540.2	1322600.1 $\pm$ 202444.2
S83	15.3	589.30	7410617.8 $\pm$ 1768536.9	7733749.0 $\pm$ 1845651.9	7768438.3 $\pm$ 1853930.4
S85	11.0	1772.21	22152053.5 $\pm$ 33765230.9	23117967.4 $\pm$ 35237523.6	23221661.8 $\pm$ 35395579.5
S87	7.6	1577.89	19792626.5 $\pm$ 1922704.9	20655660.4 $\pm$ 2006542.2	20748310.3 $\pm$ 2015542.4
S89	31.0	273.90	3439128.4 $\pm$ 474176.5	3589087.5 $\pm$ 494852.4	3605186.1 $\pm$ 497072.0
S91	11.4	891.25	11199826.5 $\pm$ 970523.3	11688181.6 $\pm$ 1012841.8	11740608.3 $\pm$ 1017384.8
S96	13.6	646.91	8134554.8 $\pm$ 512145.9	8489252.4 $\pm$ 534477.4	8527330.4 $\pm$ 536874.7
S97	9.7	1151.43	14531570.5 $\pm$ 5278240.7	15165202.3 $\pm$ 5508392.1	15233225.0 $\pm$ 5533099.7
S145	23.6	343.33	4332795.7 $\pm$ 2127712.2	4521722.1 $\pm$ 2220488.5	4542004.0 $\pm$ 2230448.4
S175	1812.0	6.30	79183.3 $\pm$ 19172.5	82636.0 $\pm$ 20008.5	83006.7 $\pm$ 20098.3
R34	18.6	589.73	7427033.2 $\pm$ 2111171.4	7750880.2 $\pm$ 2203226.5	7785646.3 $\pm$ 2213108.9
R44	5.5	2579.33	33005557.9 $\pm$ 21665177.6	34444725.9 $\pm$ 22609861.9	34599225.9 $\pm$ 22711277.1

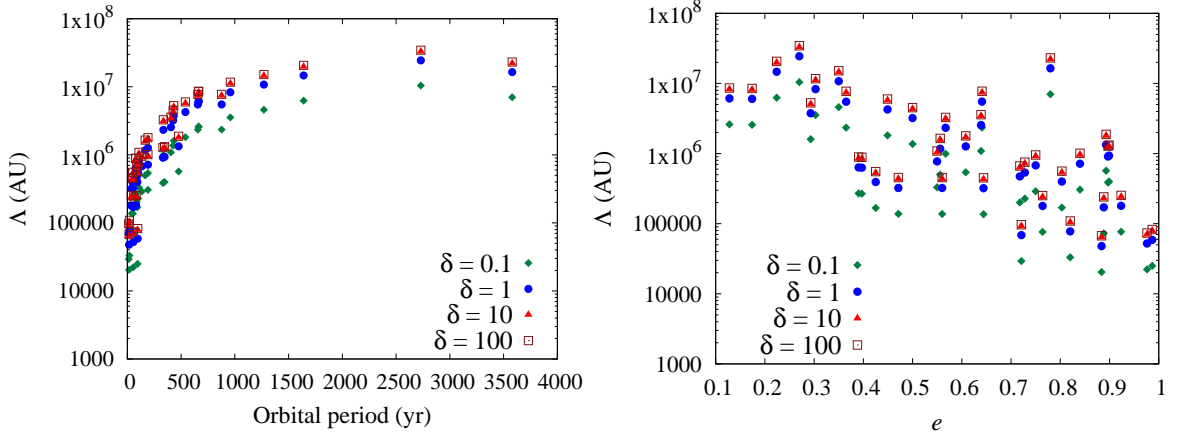


**Figure 2.** The graphic of range of interaction  $\Lambda$  vs. observed orbital period  $P$  (left) and eccentricity  $e$  (right) of S-stars for 4 different values of parameter  $\delta$  equals 0.1, 1, 10 and 100, respectively.

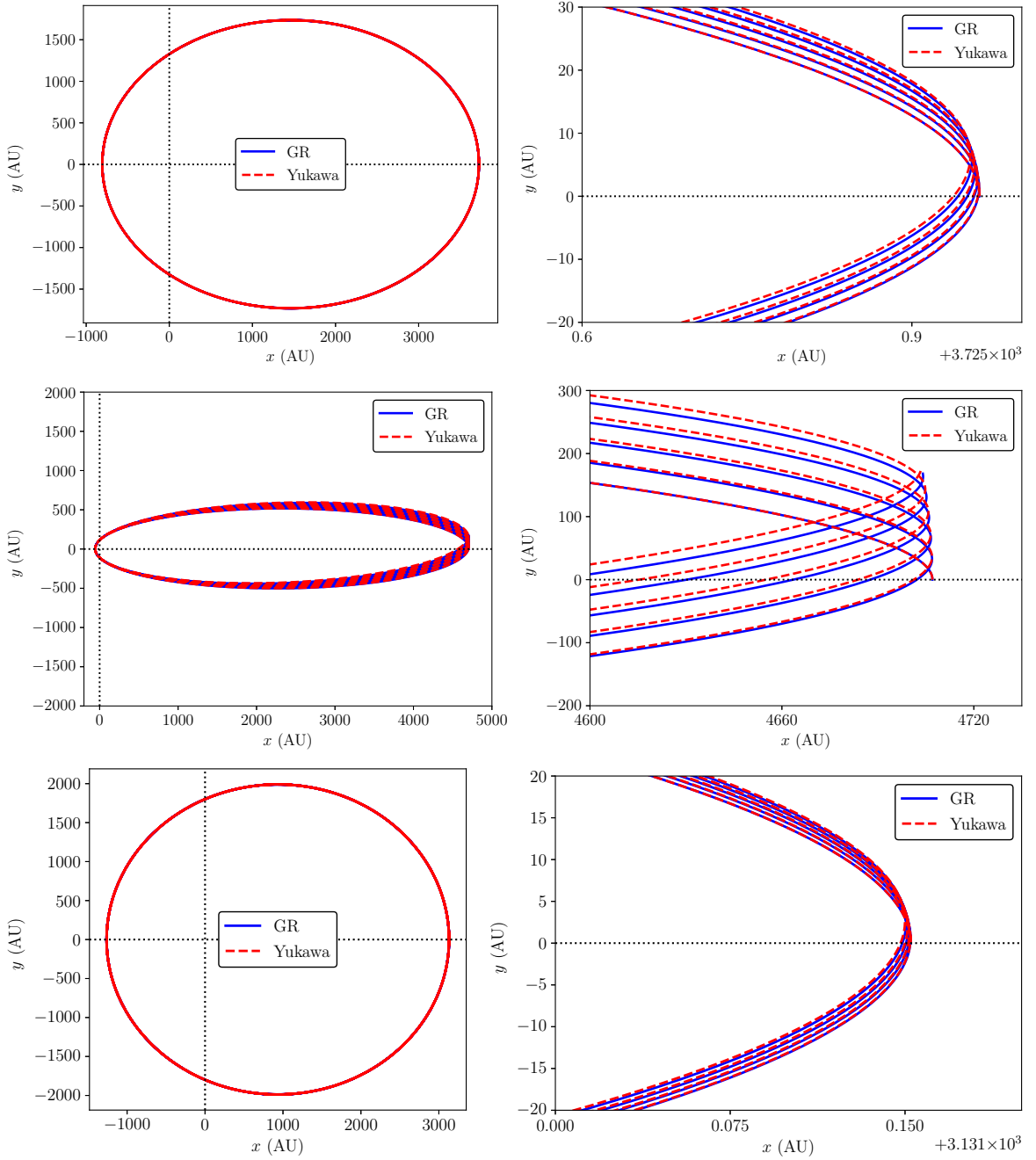
smaller values of  $\delta$ .

Fig. 3 shows comparisons between the simulated orbits of S9, S14 and S13 stars in both GR and Yukawa gravity, obtained by numerical integration of the corresponding equations of motion (3.1) and (3.2) during their five orbital periods and for  $\delta = 1$ . The left panels in Fig. 3 show the full stellar orbits, while the regions around their apocenters are zoomed in the right panels for better insight. These three stars are chosen due to their drastically different eccentricities, as well as due to their orbital periods around 50 yr, which makes these stars the good candidates for future monitoring with large observational facilities.

Periods of S9, S14 and S13 stars are  $P = 51.3, 55.3$  and  $49.0$  yr and their eccentricities are  $e = 0.644, 0.9761$ , and  $0.425$ , respectively. As it can be seen from Fig. 3, there are a small deviations between GR and Yukawa orbits in the case of these three S-stars. Orbits are obtained for  $\Lambda = 320000.8, 52205.2$  and  $393179.8$  AU, respectively. These deviations are expected [1]. Assuming that the range of Yukawa gravity  $\Lambda$  is fixed to its value corresponding to  $\delta = 1$  (e.g.  $\Lambda = 52205.2$  AU in the case of S14 star), and that instead of  $\delta = 1$  we use different values (e.g.  $\delta = 0.1, 10$  or  $1000$ ), these deviations become larger (see the case for S14 star presented in Fig. 4). The discrepancy between the simulated orbits in Yukawa gravity and in GR becomes noticeable for  $\delta > 0.1$  and rises with increase of  $\delta$  and then saturates and tends to become nearly constant for  $\delta > 1$ . Also, if  $\Lambda$  is fixed, and  $\delta$  is varied, orbits in Yukawa gravity change significantly in the range  $0.1 < \delta < 1$ . Outside of this interval for  $\delta$ , influence of  $\delta$  on S-star orbit is very small. Thus, one can conclude that the influence of strength of Yukawa interaction  $\delta$  on stellar orbits is noticeable for range  $0.1 < \delta < 1$ , especially in case of S-stars with high orbital eccentricities  $e$ .

#### 4.2 Constrains on Yukawa gravity parameters from Markov chain Monte Carlo simulations

In this subsection we estimated 68% confidence region for the Yukawa gravity parameters  $\delta$  and  $\Lambda$  using Markov chain Monte Carlo (MCMC) [118–123]. MCMC methods provide very efficient sampling approximations to the posterior probability density function in parameter spaces [118]. We used MIT licensed pure-Python implementation of Goodman & Weare’s Affine Invariant Markov chain Monte Carlo Ensemble sampler (<https://emcee.readthedocs.io/en/stable/>). The explanation of the `emcee` algorithm and its implemen-



**Figure 3.** Comparison between the simulated orbits of S9 (top), S14 (middle) and S13 star (bottom), during five orbital periods in GR (blue solid line) and in Yukawa gravity (red dashed line) for  $\delta = 1$ . The corresponding values of the range of Yukawa interaction are:  $\Lambda = 320000.8, 52205.2$  and  $393179.8$  AU, respectively. The left panels show full stellar orbits, while the regions around the apocenter are zoomed in the right panels for better insight.

tation in detail are given in [118]. We obtained the maximum likelihood values of Yukawa gravity parameters using the `optimize.minimize` module from SciPy for maximization of their likelihood function. After that we used these maximum likelihood values of the param-



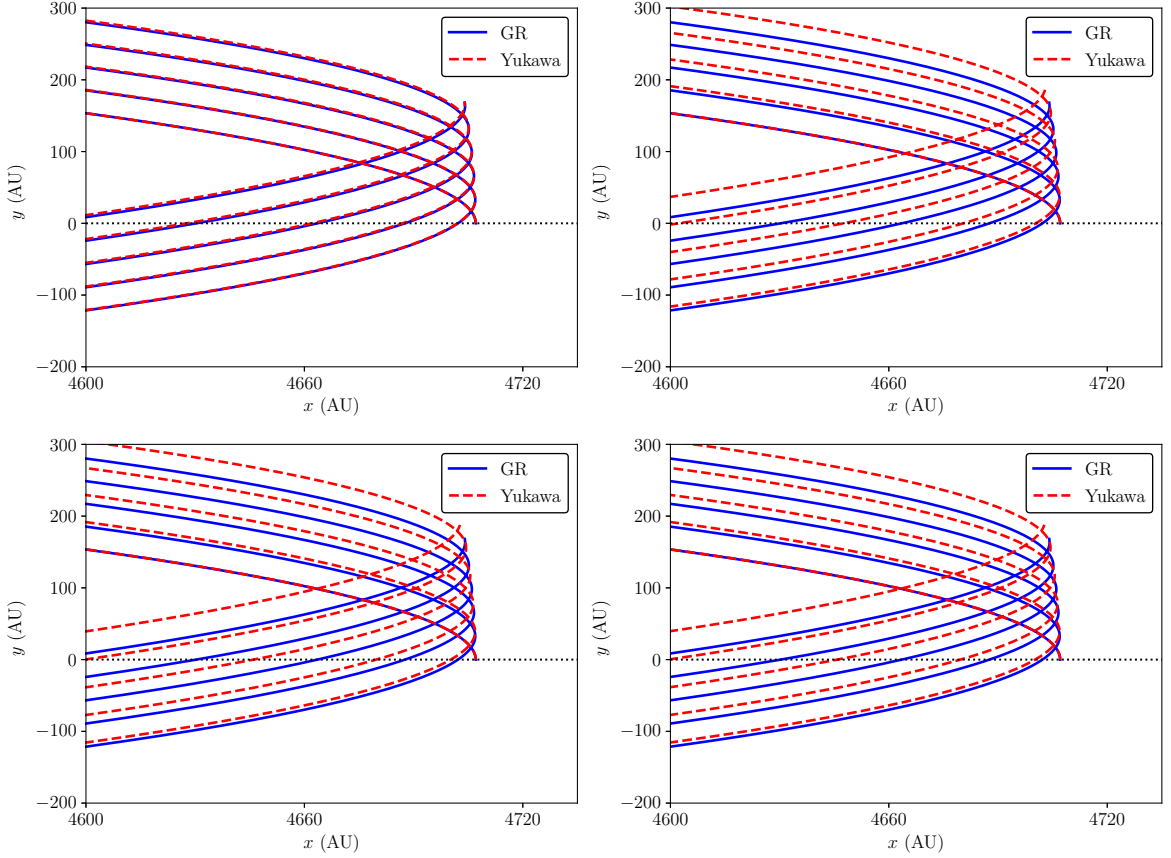


**Figure 4.** Comparisons between the simulated orbits of S14 star in GR (blue solid line) and in Yukawa gravity (red dashed line) for the following 4 different values of  $\delta$ :  $\delta = 0.1$  (top left),  $\delta = 10$  (top right),  $\delta = 100$  (bottom left) and  $\delta = 1000$  (bottom right). The orbits are calculated during five orbital periods, and their zoomed parts around the apocenter are presented for better insight. The corresponding value of  $\Lambda = 52205.2$  AU.

eters as a starting point for our MCMC simulations, which we performed in order to estimate the posterior probability distributions for the Yukawa gravity parameters. To perform these simulations, we used  $0 < \delta < 10^3$  and  $10^3 \text{AU} < \Lambda < 10^6 \text{AU}$  as our priors.

In order to test the robustness of our MCMC analysis, as well as the possible influence of the scale of each gravitational system on the obtained estimates, we performed the MCMC simulations not only for all S-stars from Table 1, but also for their following three subsamples, defined by scale criterion  $P^*$  (see Table 1 for its particular values):

1. subsample where  $5 \text{ yr} < P^* < 25 \text{ yr}$ , containing S2, S12, S14, S21, S38, S39, S55 and S175 star,
2. subsample where  $25 \text{ yr} < P^* < 50 \text{ yr}$ , containing S8, S9, S13, S18 and S23 star,
3. subsample where  $50 \text{ yr} < P^* < 100 \text{ yr}$ , containing S4, S6, S17, S19, S24, S29, S31 and S60 star.

Fig. 5 represents the obtained posterior probability distributions of the parameters of Yukawa gravity model ( $\delta$  and  $\Lambda$ ), where the contours represent their 68% confidence levels. In the case of the first subsample, the following best-fit values of Yukawa gravity parameters and

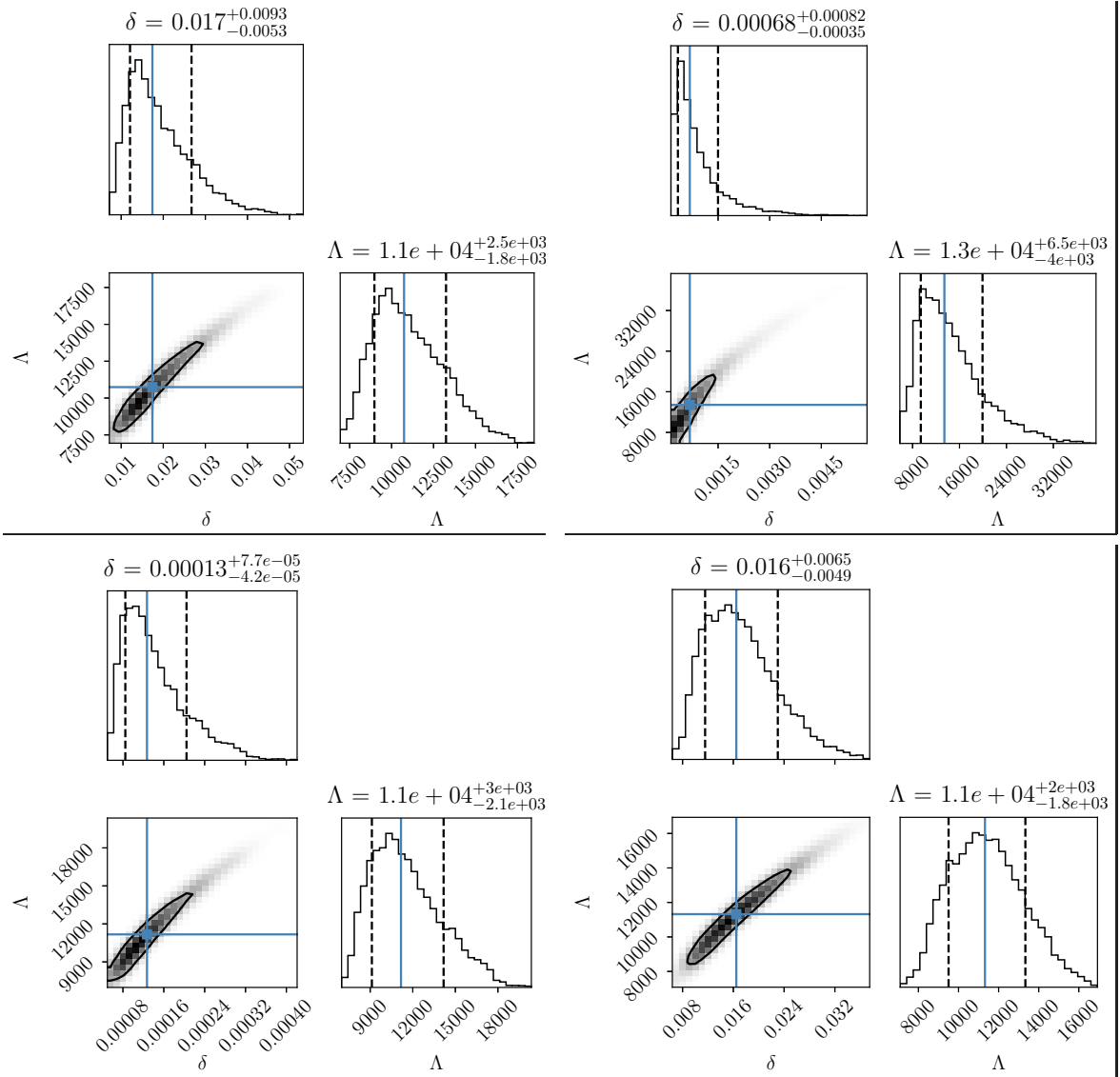


**Figure 5.** The posterior probability distributions and 68% confidence levels (closed contours) for the Yukawa gravity parameters in the case of S-stars, obtained by MCMC simulations. Top left panel corresponds to the following S-stars: S2, S12, S14, S21, S38, S39, S55 and S175, for which  $5 \text{ yr} < P^* < 25 \text{ yr}$  (see Table 1), top right panel corresponds to S8, S9, S13, S18 and S23 star for which  $25 \text{ yr} < P^* < 50 \text{ yr}$ , bottom left panel corresponds to S4, S6, S17, S19, S24, S29, S31 and S60 star for which  $50 \text{ yr} < P^* < 100 \text{ yr}$ , while bottom right panel correspond to all S-stars from Table 1. The designated best-fit values of Yukawa gravity parameters and their uncertainties were obtained from the 16th, 50th and 84th percentiles of the corresponding posterior probability distributions (vertical lines in the histograms).

their uncertainties were obtained from the 16th, 50th and 84th percentiles of the posterior probability distributions:  $\delta = 0.017^{+0.0093}_{-0.0053}$  and  $\Lambda = 11000^{+2500}_{-1800}$  AU. (see top left panel of Fig. 5). The following results were obtained in the case of the second subsample:  $\delta = 0.00068^{+0.00082}_{-0.00035}$  and  $\Lambda = 13000^{+6500}_{-4000}$  AU (see top right panel of Fig. 5), while in the case of the third subsample we got the following values:  $\delta = 0.00013^{+0.000077}_{-0.000042}$  and  $\Lambda = 11000^{+3000}_{-2100}$

AU (see bottom left panel of Fig. 5). Bottom right panel of Fig. 5 shows the corresponding results obtained for all S-stars from Table 1, in which case the following best-fit values were obtained:  $\delta = 0.016_{-0.0049}^{+0.0065}$  and  $\Lambda = 11000_{-1800}^{+2000}$  AU.

It can be seen from these results that the scale of gravitational systems also plays a significant role, since the smaller values of universal constant  $\delta$  are obtained for the subsamples of S-stars with higher values of scale criterion  $P^*$ . Therefore, the S-stars with large  $P^*$  cause that the value of  $\delta$  for whole sample (bottom right panel of Fig. 5) is slightly less than its corresponding value for the first subsample with smallest  $P^*$  (top left panel of Fig. 5). All these results obtained by MCMC simulations are consistent with our previous analyses concerning the constraints on the Yukawa gravity parameters [55, 58, 62].

Also, constraints of Yukawa gravity parameters are presented in recent following papers: [39, 52, 81, 111, 124, 125, 127]. In the references [124, 125] authors use publicly available data for the S2 star, integrated geodesics and use MCMC analysis method. They discussed the usage of S2-stars observations to constrain a Yukawa-like gravitational potential and to constrain parameter space of MODified gravity (MOG). Authors analyzed observational data and concluded that the orbital precessions of the S2 star is in good agreement with the corresponding prediction of GR. In paper [111] author performs data analysis in the framework of Yukawa gravity model by solving geodesic equation, and concluded that the orbital precessions of the S2, S38 and S55 stars are close to the corresponding prediction of GR for these stars, i.e. no significant departure from GR is detected. Results of above mentioned papers for Yukawa gravity parameters  $\delta$  and  $\Lambda$  are in good agreement with our findings from this paper (obtained using MCMC analysis of crytical period  $P^*$  for all S-stars).

In paper [39], the different graviton mass bounds obtained from massive potentials, Yukawa like and non-Yukawa like, are reviewed. The graviton mass bound from Solar System, Clusters and weak lensing with bound from gravitational waves GW150914 are compared. In Ref. [52] the solar-system data in case of Yukawa form of gravitation potential are analyzed and obtained bounds of graviton mass. There are also constrained Yukawa gravitational parameters using data from paper [126]. In paper [127] the scalar-tensor theories in the strong gravity regime around BH at the centre of our galaxy are investigated, S2 star fit is presented as well as the fit of the combined data of S2 and S38. The analysis of Yukawa gravity parameters with pulsars around Sgr A\* is given in [81].

We compare our results with another different constraints of the Yukawa parameters for some S-stars and from Solar System results. These two systems have approximately comparable scale sizes, i.e. scale of the S2 orbit is of the same order as the Solar System. In paper [52] the author presented the latest analyses of Solar System data, and showed that the best bound on  $\Lambda$  comes from the perihelion advance of Mars, giving thus the range  $\Lambda > (1.2 - 2.2) \times 10^{14}$  km depending on the specific analysis. With the calculation performed using data from Table 4 of [126], in [52] the results for range of  $\Lambda$  (all given in  $10^{14}$  km) are the following: Mercury 0.18; Venus 0.28; Earth 0.88; Mars 2.21; Jupiter 0.11 and Saturn 0.98. In reference [114] best-fit values were obtained for the parameter values of the Yukawa potential from the Solar System precession:  $\delta = 3.863_{-0.373}^{+0.373} 10^{-3}$  and  $1/\Lambda = 1.066_{-0.6074}^{+0.6074} 10^{-3}$  AU $^{-1}$ . In paper [111] best-fit values were obtained for the S2 star data:  $\delta = 0.00_{-0.36}^{+1.53}$ ,  $\Lambda \geq 7059.29$  AU; for S38 star data:  $\delta = 0.00_{-0.34}^{+1.54}$ ,  $\Lambda \geq 5731.30$  AU for S55 star data:  $\delta = -0.10_{-0.33}^{+1.62}$ ,  $\Lambda \geq 3511.95$  AU and for multi-star data:  $\delta = 0.00_{-0.52}^{+1.69}$ ,  $\Lambda \geq 6336.23$  AU. In reference [124] best-fit values were obtained for the S2 star data, by excluding and including the measurement of the orbital precession of S2 star, respectively:  $\delta \geq -0.07$ ,  $\Lambda \geq 9540$  AU, and  $\delta \geq -0.01_{-0.14}^{+0.61}$ ,  $\Lambda \geq 6300$  AU.

All these authors obtain that the range of Yukawa interaction is of the similar order of magnitude, as the results presented here.

## 5 Conclusions

We investigated the influence of strength of Yukawa interaction  $\delta$  on the observed stellar orbits of the S-stars. All of these results were obtained assuming that the precession angles of S-stars in Yukawa gravity will have a small deviation from GR prediction (as indicated by GRAVITY Collaboration [1]). We believe that Yukawa can provide a fit for the trajectories of S-stars, however assuming that in the future observations Schwarzschild precessions will be close to their GR estimates, we showed that these precessions can be fitted by a set of Yukawa gravity parameters. Our results showed the following:

- Strength of Yukawa interaction  $\delta$  strongly affects its range  $\Lambda$  and vice versa, i.e. these two gravity parameters are mutually correlated for smaller values of  $\delta$ ;
- Orbits with larger periods  $P$ , smaller eccentricities  $e$  and higher value of strength of Yukawa interaction  $\delta$  provide larger values of range of Yukawa interaction  $\Lambda$ ;
- Strength of Yukawa interaction  $\delta$  has noticeable influence on stellar orbits, especially in case of S-stars with high orbital eccentricities  $e$ . Discrepancy between Yukawa and GR simulated orbits is better visible in case of orbits with higher eccentricity  $e$ , because value of precession is then higher and it is more easy to detect discrepancy from GR orbit. However, values of  $\Lambda$  are larger for lower eccentricities  $e$ ;
- In the case of the fixed range of Yukawa interaction  $\Lambda$ , discrepancy between the simulated orbits in Yukawa gravity and in GR becomes noticeable for  $\delta > 0.1$  and rises with increase of  $\delta$  and then saturates and tends to become nearly constant for  $\delta > 1$ ;
- Our MCMC simulations resulted with the following best-fit values and uncertainties of Yukawa gravity parameters in the case of the sample of S-stars from Tables 1 and 2:  $\delta = 0.017^{+0.0093}_{-0.0053}$  and  $\Lambda = 11000^{+2500}_{-1800}$  AU.
- These MCMC simulations also demonstrated that the scale of gravitational systems plays a significant role and that it can have significant influence on the values of both Yukawa gravity parameters. S-stars which represent larger gravitational systems are better described with the lower strength of Yukawa interaction  $\delta$ , while the opposite holds for the S-stars with orbits of smaller scales.
- We defined scale criterion  $P^*$ , according to which we divided samples of all studied S-stars into three subsamples. These results showed that the scale of the gravitational system (described by  $P^*$ ) is very sensitive to the values of strength of Yukawa interaction  $\delta$ . Therefore, the quantity  $P^*$  can be used as a criterion for classification of the gravitational systems according to their scales, in the frame of Yukawa gravity.

It is very important to investigate the influence of strength on Yukawa interaction on observed stellar orbits around GC in the frame of the Yukawa-type gravity theories because it represents an excellent way for probing and testing the predictions of gravity theories. Also, we believe that our current estimates for Yukawa gravity parameters can be significantly improved with new observations of trajectories of bright stars near the Galactic Center like GRAVITY [128], E-ELT [129] and TMT [130].

## Acknowledgments

This work is supported by Ministry of Science, Technological Development and Innovations of the Republic of Serbia through the Project contracts No. 451-03-47/2023-01/200002 and 451-03-47/2023-01/200017.

## References

- [1] GRAVITY Collaboration, *Detection of the Schwarzschild precession in the orbit of the star S2 near the Galactic centre massive black hole*, *Astron. Astrophys.* **636** (2020) L5 [[arXiv:2004.07187](#)].
- [2] T. Damour, *100 Years of Relativity: Was Einstein 100 % Right?*, *AIP Conference Proceedings* **841** (2006) 51.
- [3] A. Cho, *At Long Last, Gravity Probe B Satellite Proves Einstein Right*, *Science* **332** (2011) 649.
- [4] F. De Paolis, *Never bet against Einstein*, *Int. J. Mod. Phys. D* **31** (2022) 2240014 [[arXiv:2206.06831](#)].
- [5] D. Lynden-Bell and M. J. Rees, *The Galactic Center*, *Mon. Not. R. Astron. Soc.* **152** (1971) 461.
- [6] J. H. Oort, *The Galactic Center*, *Ann. Rev. Astron. Astrophys.* **15** (1977) 295.
- [7] M. J. Rees, *The Compact source at the Galactic Center*, *AIP Conference Proceedings* **83** (1982) 166.
- [8] M. Reid, *Is There a Supermassive Black Hole at the Center of the Milky Way?* *Int. J. Mod. Phys. D* **18** (2009) 889 [[arXiv:0808.2624](#)].
- [9] F. Munyaneza and R. D. Viollier, *The Motion of Stars near the Galactic Center: A Comparison of the Black Hole and Fermion Ball Scenarios*, *Astrophys. J.* **564** (2002) 274 [[arXiv:astro-ph/0103466](#)].
- [10] P. Jetzer, *Boson stars*, *Phys. Rep.* **220** (1992) 163.
- [11] D. F. Torres, S. Capozziello and G. Lambiase, *Supermassive boson star at the galactic center?* *Phys. Rev. D* **62** (2000) 104012. [[astro-ph/0004064](#)].
- [12] F. H. Vincent, Z. Meliani, P. Grandclément, E.ourgoulhon and O. Straub, *Imaging a boson star at the Galactic center*, *Class. Quantum Grav.* **33** (2016) 105015 [[arXiv:1510.04170](#)].
- [13] R. D. Viollier, D. Trautmann, and G. B. Tupper, *Supermassive neutrino stars and galactic nuclei*, *Phys. Lett. B* **306** (1993) 79.
- [14] F. De Paolis, G. Ingrosso, A. A. Nucita, D. Orlando, S. Capozziello and G. Iovane, *Astrophysical constraints on a possible neutrino ball at the Galactic Center*, *Astron. Astrophys.* **376** (2001) 853 [[astro-ph/0107497](#)].
- [15] F. Munyaneza, D. Tsiklauri, and R. D. Viollier, *Sagittarius A\*: A supermassive black hole or a spatially extended object?* *Astrophys. J. Lett.* **509** (1998) L105 [[astro-ph/9808219](#)].
- [16] D. Tsiklauri and R. D. Viollier, *Dark matter concentration in the Galactic Center*, *Astrophys. J.* **500** (1998) 591 [[astro-ph/9805273](#)].
- [17] N. Bilić, F. Munyaneza, and R. D. Viollier, *Stars and halos of degenerate relativistic heavy-neutrino and neutralino matter*, *Phys. Rev. D* **59** (1998) 024003 [[astro-ph/9801262](#)].
- [18] N. Bilić, F. Munyaneza, G. B. Tupper, and R. D. Viollier, *The dynamics of stars near Sgr A\* and dark matter at the center and in the halo of the Galaxy*, *Prog. Part. Nucl. Phys.* **48** (2002) 291.

- [19] K.S. Virbhadra, *Relativistic images of Schwarzschild black hole lensing*, *Phys. Rev. D* **79** (8) (2009) 083004.
- [20] R. Ruffini, C. R. Argüelles, and J. A. Rueda, *On the core-halo distribution of dark matter in galaxies*, *Mon. Not. R. Astron. Soc.* **451** (2015) 622 [[arXiv:1409.7365](#)].
- [21] E. A. Becerra-Vergara, C. R. Argüelles, A. Krut, J. A. Rueda, and R. Ruffini, *Hinting a dark matter nature of Sgr A\* via the S-stars*, *Mon. Not. R. Astron. Soc. Lett.* **505** (2021) L64 [[arXiv:2105.06301](#)].
- [22] A. F. Zakharov, *Testing the Galactic Centre potential with S-stars*, *Mon. Not. R. Astron. Soc. Lett.* **511** (2022) L35 [[arXiv:2108.09709](#)].
- [23] A. F. Zakharov, *Orbits of Bright Stars Near the Galactic Center as a Tool to Test Gravity Theories*, *Moscow Univ. Phys. Bull.* **77** (2022) 341.
- [24] C. R. Argüelles, M. F. Mestre, E. A. Becerra-Vergara, V. Crespi, A. Krut, J. A. Rueda and R. Ruffini, *What does lie at the Milky Way centre? Insights from the S2-star orbit precession*, *Mon. Not. R. Astron. Soc. Lett.* **511** (2022) L35 [[arXiv:2109.10729](#)].
- [25] J. Bardeen, *Timelike and null geodesics in the Kerr metric*, in *Black Holes (Les Astres Occlus)*, eds. B. S. DeWitt and C. DeWitt-Morette, New York: Gordon & Breach, 1973, p. 215.
- [26] S. Chandrasekhar, *Mathematical Theory of Black Holes*, Oxford: Clarendon Press, 1983.
- [27] H. Falcke, F. Melia and E. Agol, *Viewing the Shadow of the Black Hole at the Galactic Center*, *Astrophys. J. Lett.* **528** (2000) L13.
- [28] F. Melia and H. Falcke, *The Supermassive Black Hole at the Galactic Center*, *Ann. Rev. in Astron. Astrophys.* **39** (2001) 309.
- [29] A. Eckart and R. Genzel, *Observations of stellar proper motions near the Galactic Centre*, *Nature* **383** (1996) 415.
- [30] A. M. Ghez, B. L. Klein, M. Morris and E. E. Becklin, *High Proper-Motion Stars in the Vicinity of Sagittarius A\*: Evidence for a Supermassive Black Hole at the Center of Our Galaxy*, *Astrophys. J.* **509** (1998) 678.
- [31] A. F. Zakharov, A. A. Nucita, F. De Paolis, and G. Ingrosso, *Measuring the black hole parameters in the galactic center with RADIOASTRON*, *New Astron.* **10** (2005) 479 [[astro-ph/0411511](#)].
- [32] A. F. Zakharov, F. De Paolis, G. Ingrosso and A. A. Nucita, *Direct measurements of black hole charge with future astrometrical missions*, *Astron. Astrophys.* **442** (2005) 795 [[astro-ph/0505286](#)].
- [33] Event Horizon Telescope Collaboration: K. Akiyama, A. Alberdi, W. Alef et al., *First M87 Event Horizon Telescope Results. I. The Shadow of the Supermassive Black Hole* *Astrophys. J. Lett.* **875** (2019) L1.
- [34] Event Horizon Telescope Collaboration: K. Akiyama, A. Alberdi, W. Alef et al., *First Sagittarius A\* Event Horizon Telescope Results. I. The Shadow of the Supermassive Black Hole in the Center of the Milky Way*, *Astrophys. J. Lett.* **930** (2022) L12.
- [35] GRAVITY Collaboration, *Detection of the gravitational redshift in the orbit of the star s2 near the galactic centre massive black hole*, *Astron. Astrophys.* **615** (2018) L15 [[arXiv:1807.09409](#)].
- [36] GRAVITY Collaboration, *A geometric distance measurement to the Galactic Center black hole with 0.3% uncertainty*, *Astron. Astrophys.* **625** (2019) L10 [[arXiv:1904.05721](#)].
- [37] T. Do, A. Hees, A. Ghez, G.D. Martinez, D.S. Chu, S. Jia et al., *Relativistic redshift of the star S0-2 orbiting the Galactic Center supermassive black hole*, *Science* **365** (2019) 664 [[arXiv:1907.10731](#)].



- [38] C. de Rham, *Massive gravity*, *Liv. Rev. Relat.* **17** (2014) 7 [[arXiv:1401.4173](#)].
- [39] C. de Rham, J.T. Deskins, A.J. Tolley and S.-Y. Zhou, *Graviton mass bounds*, *Rev. Mod. Phys.* **89** (2017) 025004 [[arXiv:1606.08462](#)].
- [40] E. Babichev, C. Deffayet and R. Ziour, *Recovering General Relativity from massive gravity*, *Phys. Rev. Lett.* **103** (2009) 201102 [[arXiv:0907.4103](#)].
- [41] D. G. Boulware and S. Deser, *Can Gravitation Have a Finite Range?* *Phys. Rev. D* **6** (1972) 3368.
- [42] M. Fierz and W. Pauli, *On relativistic wave equations for particles of arbitrary spin in an electromagnetic field*, *Proc. R. Soc. London Series A* **173** (1939) 211.
- [43] C.M. Will, *Bounding the mass of the graviton using gravitational-wave observations of inspiralling compact binaries*, *Phys. Rev. D* **57** (1998) 2061 [[gr-qc/9709011](#)].
- [44] C.M. Will, *The confrontation between general relativity and experiment*, *Liv. Rev. Relativity* **17** (2014) 4 [[arXiv:1403.7377](#)].
- [45] R.H. Sanders, *Anti-gravity and galaxy rotation curves*, *Astron. Astrophys.* **136** (1984) L21.
- [46] E. G. Adelberger, J. H. Gundlach, B. R. Heckel, S. Hoedl and S. Schlamminger, *Torsion balance experiments: A low-energy frontier of particle physics*, *Progr. Part. Nucl. Phys.* **62** (2009) 102.
- [47] LIGO Scientific Collaboration and Virgo Collaboration, *Observation of Gravitational Waves from a Binary Black Hole Merger*, *Phys. Rev. Lett.* **116** (2016) 061102 [[arXiv:1602.03837](#)].
- [48] LIGO Scientific Collaboration and Virgo Collaboration, *Tests of general relativity with GW150914*, *Phys. Rev. Lett.* **116** (2016) 221101 [[arXiv:1602.03841](#)].
- [49] LIGO Scientific Collaboration, Virgo Collaboration and KAGRA collaboration, *Tests of General Relativity with GWTC-3*, [[arXiv:2112.06861](#)].
- [50] K. Lee, F.A. Jenet, R.H. Price, N. Wex and M. Kramer, *Detecting massive gravitons using pulsar timing arrays*, *Astrophys. J.* **722** (2010) 1589 [[arXiv:1008.2561](#)].
- [51] A. Rana, D. Jain, S. Mahajan and A. Mukherjee, *Bounds on graviton mass using weak lensing and SZ effect in galaxy clusters*, *Phys. Lett. B* **781** (2018) 220 [[arXiv:1801.03309](#)].
- [52] C.M. Will, *Solar system versus gravitational-wave bounds on the graviton mass*, *Class. Quant. Grav.* **35** (2018) 17LT01 [[arXiv:1805.10523](#)].
- [53] LIGO Scientific Collaboration and Virgo Collaboration, (*Fermi* Gamma-ray Burst Monitor) and (*INTEGRAL*), *Gravitational waves and gamma-rays from a binary neutron star merger: GW170817 and GRB170817a*, *Astrophys. J. Lett.* **848** (2017) L13 [[arXiv:1710.05834](#)].
- [54] LIGO Scientific Collaboration and Virgo Collaboration, *Fermi* Gamma-ray Burst Monitor, *INTEGRAL* et al., *Multi-messenger Observations of a Binary Neutron Star Merger*, *Astrophys. J. Lett.* **848** (2017) L12 [[arXiv:1710.05833](#)].
- [55] D. Borka, P. Jovanović, V. Borka Jovanović and A.F. Zakharov, *Constraining the range of Yukawa gravity interaction from S2 star orbits*, *JCAP* **11** (2013) 050 [[arXiv:1311.1404](#)].
- [56] S. Capozziello, D. Borka, P. Jovanović and V. Borka Jovanović, *Constraining extended gravity models by S2 star orbits around the Galactic Centre*, *Phys. Rev. D* **90** (2014) 044052 [[arXiv:1408.1169](#)].
- [57] P. Jovanović, D. Borka, V. Borka Jovanović and A.F. Zakharov, *Influence of bulk mass distribution on orbital precession of S2 star in Yukawa gravity*, *Eur. Phys. J. D* **75** (2021) 145 [[arXiv:2105.03403](#)].
- [58] A.F. Zakharov, P. Jovanović, D. Borka and V. Borka Jovanović, *Constraining the range of Yukawa gravity interaction from S2 star orbits II: bounds on graviton mass*, *JCAP* **04** (2016) 045 [[arXiv:1605.00913](#)].

- [59] A. Zakharov, P. Jovanović, D. Borka and V. Borka Jovanović, *Trajectories of bright stars at the Galactic Center as a tool to evaluate a graviton mass*, *Eur. Phys. J. Web of Conf.* **125** (2016) 01011 (8pp.).
- [60] A. F. Zakharov, P. Jovanović, D. Borka and V. Borka Jovanović, *Graviton mass evaluation with trajectories of bright stars at the galactic center*, *J. Phys. Conf. Ser.* **798** (2017) 012081 (5pp.).
- [61] A. Zakharov, P. Jovanović, D. Borka and V. Borka Jovanović, *Graviton mass bounds from an analysis of bright star trajectories at the galactic center*, *Eur. Phys. J. Web of Conf.* **138** (2017) 01010 (10pp.).
- [62] A. F. Zakharov, P. Jovanović, D. Borka and V. Borka Jovanović, *Constraining the range of yukawa gravity interaction from S2 star orbits III: improvement expectations for graviton mass bounds*, *JCAP* **04** (2018) 050 [[arXiv:1801.04679](#)].
- [63] A. F. Zakharov, P. Jovanović, D. Borka and V. Borka Jovanović, *Different ways to estimate graviton mass*, *Intern. J. Mod. Phys. Conf. Ser.* **47** (2018) 1860096 (7pp.) [[arXiv:1712.08339](#)].
- [64] A. M. Ghez, S. Salim, N. N. Weinberg, J. R. Lu, T. Do, J. K. Dunn et al., *Measuring distance and properties of the Milky Way's central supermassive black hole with stellar orbits*, *Astrophys. J.* **689** (2008) 1044 [[arXiv:0808.2870](#)].
- [65] S. Gillessen, F. Eisenhauer, T.K. Fritz, H. Bartko, K. Dodds-Eden, O. Pfuhl et al., *The Orbit of the Star S2 Around Sgr A\* from Very Large Telescope and Keck Data*, *Astrophys. J.* **707** (2009) L114 [[arXiv:0910.3069](#)].
- [66] S. Gillessen, F. Eisenhauer, S. Trippe, T. Alexander, R. Genzel, F. Martins et al., *Monitoring stellar orbits around the massive black hole in the galactic center*, *Astrophys. J.* **692** (2009) 1075 [[arXiv:0810.4674](#)].
- [67] S. Gillessen, P.M. Plewa, F. Eisenhauer, R. Sari, I. Waisberg, M. Habibi et al., *An update on monitoring stellar orbits in the galactic center*, *Astrophys. J.* **837** (2017) 30 [[arXiv:1611.09144](#)].
- [68] A. Hees, T. Do, A. M. Ghez, G. D. Martinez, S. Naoz, E. E. Becklin et al., *Testing General Relativity with Stellar Orbits around the Supermassive Black Hole in Our Galactic Center*, *Phys. Rev. Lett.* **118** (2017) 211101 [[arXiv:1705.07902](#)].
- [69] D.S. Chu, T. Do, A. Hees, A. Ghez, S. Naoz, G. Witzel et al., *Investigating the Binarity of S0-2: Implications for Its Origins and Robustness as a Probe of the Laws of Gravity around a Supermassive Black Hole*, *Astrophys. J.* **854** (2018) 12 [[arXiv:1709.04890](#)].
- [70] GRAVITY Collaboration, *Scalar field effects o the orbit of S2 star*, *Mon. Not. R. Astron. Soc.* **489** (2019) 4606 [[arXiv:1908.06681](#)].
- [71] A. Hees, T. Do, B.M. Roberts, A.M. Ghez, S. Nishiyama, R.O. Bentley et al., *Search for a Variation of the Fine Structure Constant around the Supermassive Black Hole in Our Galactic Center*, *Phys. Rev. Lett.* **124** (2020) 081101 [[arXiv:2002.11567](#)].
- [72] Particle Data Group, *Review of particle physics*, *Progr. Theor. Exper. Phys.* **2022** (2022) 083C01..
- [73] C. Talmadge, J. P. Berthias, R. W. Hellings and E. M. Standish, *Model-independent constraints on possible modifications of Newtonian gravity*, *Phys. Rev. Lett.* **61** (1988) 1159.
- [74] M. Sereno and P. Jetzer, *Dark matter versus modifications of the gravitational inverse-square law: results from planetary motion in the Solar system*, *Mon. Not. R. Astron. Soc.* **371** (2006) 626 [[astro-ph/0606197](#)].
- [75] V. F. Cardone and S. Capozziello, *Systematic biases on galaxy haloes parameters from Yukawa-like gravitational potentials*, *Mon. Not. R. Astron. Soc.* **414** (2011) 1301 [[arXiv:1102.0916](#)].

- [76] L. Iorio, *Constraints on the range  $\lambda$  of Yukawa-like modifications to the Newtonian inverse-square law of gravitation from Solar System planetary motions*, *JHEP* **2007** (2007) 041 [[arXiv:0708.1080](#)].
- [77] L. Iorio, *Putting Yukawa-Like Modified Gravity (MOG) on the Test in the Solar System*, *Schol. Res. Exchange* **2008** (2008) 8385 [[arXiv:0809.3563](#)].
- [78] S. Capozziello, A. Stabile and A. Troisi, *Newtonian limit of  $f(R)$  gravity*, *Phys. Rev. D* **76** (2007) 104019 [[arXiv:0708.0723](#)].
- [79] S. Capozziello, E. de Filippis and V. Salzano, *Modelling clusters of galaxies by  $f(R)$  gravity*, *Mon. Not. R. Astron. Soc.* **394** (2009) 947 [[arXiv:0809.1882](#)].
- [80] X. Miao, L. Shao, and B.-Q. Ma, *Bounding the mass of graviton in a dynamic regime with binary pulsars*, *Phys. Rev. D* **99** (2019) 123015.
- [81] Y. Dong, L. Shao, Z. Hu, X. Miao and Z. Wang, *Prospects for constraining the Yukawa gravity with pulsars around Sagittarius A\**, *JCAP* **2022**, No. 11 (2022) 051 [[arxiv:2210.16130](#)].
- [82] M. White and C.S. Kochanek, *Constraints on the Long-Range Properties of Gravity from Weak Gravitational Lensing*, *Astrophys. J.* **560** (2001) 539 [[astro-ph/0105227](#)].
- [83] L. Amendola and C. Quercellini, *Skewness as a Test of the Equivalence Principle*, *Phys. Rev. Lett.* **92** (2004) 181102 [[astro-ph/0403019](#)].
- [84] S. Reynaud and M.-T. Jaekel, *Testing the Newton Law at Long Distances*, *Int. J. Mod. Phys. A* **20** (2005) 2294 [[gr-qc/0501038](#)].
- [85] C. Sealfon, L. Verde and R. Jimenez, *Limits on deviations from the inverse-square law on megaparsec scales*, *Phys. Rev. D* **71** (2005) 083004 [[astro-ph/0404111](#)].
- [86] J. W. Moffat, *Gravitational theory, galaxy rotation curves and cosmology without dark matter*, *JCAP* **05** (2005) 003 [[astro-ph/0412195](#)].
- [87] J.W. Moffat, *Scalar tensor vector gravity theory*, *JCAP* **03** (2006) 004 [[gr-qc/0506021](#)].
- [88] A. Stabile and S. Capozziello, *Galaxy rotation curves in  $f(R, \phi)$  gravity*, *Phys. Rev. D* **87** (2013) 064002 [[arXiv:1302.1760](#)].
- [89] D. Borka, P. Jovanović, V.B. Jovanović and A.F. Zakharov, *Constraints on  $R^n$  gravity from precession of orbits of  $S_2$ -like stars*, *Phys. Rev. D* **85** (2012) 124004 [[arXiv:1206.0851](#)].
- [90] A.F. Zakharov, D. Borka, V. Borka Jovanović and P. Jovanović, *Constraints on  $R^n$  gravity from precession of orbits of  $S_2$ -like stars: A case of a bulk distribution of mass*, *Adv. Space Res.* **54** (2014) 1108 [[arXiv:1407.0366](#)].
- [91] D. Borka, S. Capozziello, P. Jovanović and V. Borka Jovanović, *Probing hybrid modified gravity by stellar motion around Galactic Center*, *Astropart. Phys.* **79** (2016) 41 [[arXiv:1504.07832](#)].
- [92] K. F. Dialektopoulos, D. Borka, S. Capozziello, V. Borka Jovanović and P. Jovanović, *Constraining nonlocal gravity by  $S_2$  star orbits*, *Phys. Rev. D* **99** (2019) 044053 [[arXiv:1812.09289](#)].
- [93] V. Borka Jovanović, P. Jovanović, D. Borka, S. Capozziello, S. Gravina and A. D’Addio, *Constraining Scalar-Tensor gravity models by  $S_2$  star orbits around the Galactic Center*, *Facta Universitatis: Series Phys. Chem. Tech.* **17** (2019) 11 [[arXiv:1904.05558](#)].
- [94] V. Borka Jovanović, S. Capozziello, P. Jovanović and D. Borka, *Recovering the fundamental plane of galaxies by  $f(R)$  gravity*, *Phys. Dark Universe* **14** (2016) 73.
- [95] S. Capozziello, V. Borka Jovanović, D. Borka and P. Jovanović, *Constraining theories of gravity by fundamental plane of elliptical galaxies*, *Phys. Dark Universe* **29** (2020) 100573 [[arXiv:2004.11557](#)].

- [96] V. Borka Jovanović, D. Borka, P. Jovanović and S. Capozziello, *Possible effects of hybrid gravity on stellar kinematics in elliptical galaxies*, *Eur. Phys. J. D* **75** (2021) 149 [[arXiv:2105.03357](#)].
- [97] S. Capozziello, P. Jovanović, V. Borka Jovanović and D. Borka, *Addressing the missing matter problem in galaxies through a new fundamental gravitational radius*, *JCAP* **06** (2017) 044 [[arXiv:1702.03430](#)].
- [98] A. M. Ghez, M. Morris, E. E. Becklin, A. Tanner and T. Kremenek, *The accelerations of stars orbiting the Milky Way's central black hole*, *Nature* **407** (2000) 349 [[astro-ph/0009339](#)].
- [99] R. Schödel, T. Ott, R. Genzel, R. Hofmann, M. Lehnert, A. Eckart et al., *A star in a 15.2-year orbit around the supermassive black hole at the centre of the Milky Way*, *Nature* **419** (2002) 694 [[astro-ph/0210426](#)].
- [100] R. Genzel, F. Eisenhauer and S. Gillessen, *The Galactic Center massive black hole and nuclear star cluster*, *Rev. Mod. Phys.* **82** (2010) 3121 [[arXiv:1006.0064](#)].
- [101] L. Meyer, A.M. Ghez, R. Schödel, S. Yelda, A. Boehle, J.R. Lu et al., *The Shortest-Known-Period Star Orbiting Our Galaxy's Supermassive Black Hole*, *Science* **338** (2012) 84 [[arXiv:1210.1294](#)].
- [102] GRAVITY Collaboration, *Mass distribution in the Galactic Center based on interferometric astrometry of multiple stellar orbits*, *Astron. Astrophys.* **657** (2022) L12 [[arXiv:2112.07478](#)].
- [103] M. Parsa, A. Eckart, B. Shahzamanian, V. Karas, M. Zajaček, J. A. Zensus et al., *Investigating the Relativistic Motion of the Stars Near the Supermassive Black Hole in the Galactic Center*, *Astrophys. J.* **845** (2017) 22 [[arXiv:1708.03507](#)].
- [104] F. Peißker, A. Eckart and M. Parsa, *S62 on a 9.9 yr orbit around Sgr A\**, *Astrophys. J.* **889** (2020) 61 [[arXiv:2002.02341](#)].
- [105] S. Kalita, *The Galactic Center Black Hole, Sgr A\*, as a Probe of New Gravitational Physics with the Scalaron Fifth Force*, *Astrophys. J.* **893** (2020) 31.
- [106] P. C. Lalremruati and S. Kalita, *Periastron shift of compact stellar orbits from general relativistic and tidal distortion effects near Sgr A\**, *Mon. Not. R. Astron. Soc.* **502** (2021) 3761.
- [107] P.C. Lalremruati and S. Kalita, *Is It Possible to See the Breaking Point of General Relativity near the Galactic Center Black Hole? Consideration of Scalaron and Higher-dimensional Gravity*, *Astrophys. J.* **925** (2022) 126.
- [108] V. I. Dokuchaev and Y. N. Eroshenko, *Physical laboratory at the center of the Galaxy*, *Phys. Uspekhi* **58** (2015) 772 [[arXiv:1512.02943](#)].
- [109] I. De Martino, R. Lazkoz and M. De Laurentis, *Analysis of the Yukawa gravitational potential in  $f(R)$  gravity I: Semiclassical periastron advance*, *Phys. Rev. D* **97** (2018) 104067 [[arXiv:1801.08135](#)].
- [110] M. De Laurentis, I. De Martino and R. Lazkoz, *Analysis of the Yukawa gravitational potential in  $f(R)$  gravity. II. Relativistic periastron advance*, *Phys. Rev. D* **97** (2018) 104068 [[arXiv:1801.08136](#)].
- [111] A. D'Addio, *S-star dynamics through a Yukawa-like gravitational potential*, *Phys. Dark Universe* **33** (2021) 100871.
- [112] D. Borka, S. Capozziello, V. Borka Jovanović, A. F. Zakharov and P. Jovanović *Estimating the Parameters of Extended Gravity Theories with the Schwarzschild Precession of S2, S38*, *Universe* **7** (2021) 407 [[arXiv:2111.00578](#)].
- [113] D. Borka, V. Borka Jovanović, V. N. Nikolić, N. Dj. Lazarov and P. Jovanović, *Estimating the Parameters of the Hybrid Palatini Gravity Model with the Schwarzschild Precession of S2, S38 and S55 Stars: Case of Bulk Mass Distribution*, *Universe* **8** (2022) 70 [[arXiv:2205.02608](#)].

- [114] D. Benisty, *Testing modified gravity via Yukawa potential in two body problem: Analytical solution and observational constraints*, *Phys. Rev. D* **106** (2022) 043001 [[arXiv:2207.08235](#)].
- [115] R. I. Gainutdinov, *PPN Motion of S-Stars Around Sgr A*, *Astrophysics* **63**, no. 4 (2020) 470-481.
- [116] T. Clifton, *Parametrized post-Newtonian limit of fourth-order theories of gravity*, *Phys. Rev. D* **77** (2008), 024041
- [117] J. Alsing, E. Berti, C. M. Will and H. Zaglauer, *Gravitational radiation from compact binary systems in the massive Brans-Dicke theory of gravity*, *Phys. Rev. D* **85** (2012) 064041.
- [118] D. Foreman-Mackey, D.W. Hogg, D. Lang and J. Goodman, *emcee: The MCMC Hammer*, *Publ. Astron. Soc. Pacific* **125(925)** (2013) 306 [[arXiv:1202.3665](#)].
- [119] B. Audren, J. Lesgourgues, K. Benabed and S. Prunet, *Conservative constraints on early cosmology with MONTE PYTHON*, *JCAP* **02** (2013) 001 [[arXiv:1210.7183](#)].
- [120] S. Sharma, *Markov Chain Monte Carlo Methods for Bayesian Data Analysis in Astronomy*, *Ann. Rev. Astron. Astrophys.* **55(1)** (2017) 213 [[arXiv:1706.01629](#)].
- [121] D. W. Hogg and D. Foreman-Mackey, *Data Analysis Recipes: Using Markov Chain Monte Carlo*, *Astrophys. J. Suppl. Ser.*, **236(1)** (2018) 11 [[arXiv:1710.06068](#)].
- [122] D. Borka, V. Borka Jovanović, S. Capozziello and P. Jovanović, *Velocity distribution of elliptical galaxies in the framework of Non-local Gravity model*, *Adv. Space Res.* (2022) <https://doi.org/10.1016/j.asr.2022.08.060>.
- [123] D. W. Hogg, J. Bovy and D. Lang, *Data analysis recipes: Fitting a model to data*, [[arXiv:1008.4686](#)].
- [124] I. De Martino, R. della Monica and M. De Laurentis, *f(R)-gravity after the detection of the orbital precession of the S2 star around the Galactic centre massive black hole*, *Phys. Rev. D* **104** (2021) L101502 [[arxiv:2106.06821](#)].
- [125] R. della Monica, I. De Martino and M. De Laurentis, *Constraining MODified Gravity with the S2 star*, *Universe* **8** (2022) 137 [[arxiv:2206.12699](#)].
- [126] E. V. Pitjeva and N. P. Pitjev, *Relativistic effects and dark matter in the Solar system from observations of planets and spacecraft*, *Mon. Not. R. Astron. Soc.* **432** (2013) 3431-3437.
- [127] D. Benisty and A.-C. Davis, *Dark energy interactions near the Galactic Center*, *Phys. Rev. D* **105** (2022) 024052 [[arxiv:2108.06286](#)].
- [128] N. Blind, F. Eisenhauer, S. Gillessen, Y. Kok, M. Lippa, G. Perrin et al., *GRAVITY: the VLTI 4-beam combiner for narrow-angle astrometry and interferometric imaging*, [[arXiv:1503.07303](#)].
- [129] European Extremely Large Telescope. Science Working Group, *An Expanded View of the Universe: Science with the European Extremely Large Telescope*, European Southern Observatory, Germany (2010).
- [130] W. Skidmore, TMT International Science Development Teams and T. Science Advisory Committee, *Thirty Meter Telescope Detailed Science Case: 2015*, *Res. Astron. Astrophys.* **15** (2015) 1945 [[arXiv:1505.01195](#)].